# ACOUSTIC EMISSION SOURCE LOCATION IN FIBRE-REINFORCED COMPOSITE MATERIALS

**Dr John Summerscales CEng, CEnv, CSci**

Advanced Composites Manufacturing Centre
School of Marine Science and Engineering
Faculty of Science and Environment
Plymouth University,
Drake Circus, Plymouth PL4 8AA, England.

**This monograph reviews calibration sources for acoustic emission (AE), source location (SL) philosophies and the application of AESL to defect and/or damage location in both isotropic and anisotropic materials and structures. The text was initially compiled circa 1993 as a chapter for a potential book which was abandoned. Selected subsequent papers on AESL (and related topics) are reviewed at this webpage.**



**Advanced Composites Manufacturing Centre at Plymouth University, 2013. ISBN 978-1-870918-04-6.**

**Contents**

## 1 INTRODUCTION

The acoustic emission (AE) from materials prior to and during damage is useful as a warning of impending failure. Deformation of the material generates short impulsive stress waves which can be detected at the surface by suitable instrumentation. The literature on acoustic emission from fibre composites has been reviewed by Arrington [1]. Drouillard has compiled comprehensive bibliographies on acoustic emission [2, 3].

It is often necessary to know the location of the acoustic emission source, especially during proof testing. This can be accomplished in a manner similar to that used by seismologists to locate the epicentre of an earthquake. A number of transducers on the surface of the component are monitored for the relative arrival times of the wavefront propagating in the test sample. The use of acoustic emission for source location, both in theory and in practice, has been summarised in an excellent booklet by Rindorf [5].

Chretien [6] proposed that two criteria should be met for successful acoustic emission source location:

- that the source has a much smaller volume than the dimensions of the structure, and
- that the signal from the source is very rapid

Based on such conditions, the continuous signals from plastic deformation are not suitable for flaw location, but the burst-type emissions from crack initiation and propagation do fulfil the criteria.

## 2 CALIBRATION SOURCES FOR ACOUSTIC EMISSION SYSTEMS

### 2.1 Breaking pencil leads

A reproducible acoustic emission simulator was developed by Nielsen [7, 8] and adopted as a standard by the European Working Group on Acoustic Emission (EWGAE) [9]. This involves breaking a 0.5 mm 2H propelling pencil lead using a special collar. A similar simulator was described by Hsu [10] and adopted as a standard by ASTM [11, 12]. However, in the ASME standard [13] the size of the lead is changed to 0.3 mm diameter.

The strength of 0.5 mm diameter 2H Pentel leads has not been constant [14] rising from 36.3 g in 1974 to a peak of 60.0 g in 1981 due to changes in the characteristics and manufacturing methods. The character of the simulated AE source has also changed. The Japanese Acoustic Emission Working Group (JAEWG) has arranged to supply standard pencil lead with very similar strength and AE signal characteristics to the lead produced in 1975 [15]. The breaking of pencil leads has been modelled by Cowin [16].

Eitzen *et al* [17] adapted the Hsu source using a load cell whose output is monitored by a peak hold device to give an absolute force input for the simulated AE from the lead break source.

### 2.2 Fracture of a glass capillary

Breckenridge *et al* [18] used a short length of thin-walled 150 μm diameter glass capillary, slowly compressed to failure by a threaded indenter, as a source of standard events. The rise time (10-90 %) was less than 100 ns. The resulting stress wave has been solved by Lamb [19] and graphical results presented by Pekeris [20]. The waveform takes the form of a pseudo-delta-velocity function with a relatively flat frequency range from 100k - 1M Hz.

Breckenridge [21] has described the NBS transducer-calibration scheme based on the above theory to obtain exact dynamic solutions to certain problems involving an elastic solid body driven by a point force. The step-function force was generated by breaking a glass capillary against the plane surface of a large circular steel cylinder. The displacement-time response at the transducer location was calculated. The frequency response of the transducer could be measured with a precision of 10%. The procedure has been adopted by ASTM [22].

### 2.3 Grinding of powders

Chambers and Hoenig [23] generated "white" noise by the fracture of small (254 μm) diameter silicon carbide particles between a steel rotating plunger and a quartz or aluminium anvil. A similar acoustic noise generator was used by Graham [24] to determine the broadband frequency responses of acoustic emission transducers. The set-up consisted of a 100 mm square 13 mm thick steel plate with a recess ground in the centre of one face. The end of a 10 mm diameter fused silica rod mounted in a PTFE bushing was rotated in the recess at speeds up to 1 Hz by a motor. Silicon carbide particles (31 μm diameter, #80 grit) were fed into the recess and fractured by the grinding action of the rod to produce simulated acoustic emission signals.

## 2.4 Ball drop

Kamio [25] used drop impact as a constant AE source and attempted to approximate the area of a crack to the AE from a falling steel ball. Tatro [26] described an experiment in which a steel ball was dropped onto the end of a straight rod instrumented with a strain gauge at the mid-section and an AE transducer on the other end. The ball produced a stress pulse with a rise time of less than 10 μs.

Dreiman [27] created forced oscillations in the sample using a device to control the impact force and point of impingement. A modified device was proposed as a calibrated AE source. Kanno *et al* [28] calibrated AE energy against steel ball drop. The frequency is approximately inversely proportional to the diameter of the ball, and independent of the drop height and plate thickness. The amplitude is proportional to a 2/3 power of the drop height. The results were explained by a theory on rebound height.

Farrow and Darby [29] simulated AE events in unidirectional CFRP using either the Hsu-Nielsen lead break source or a 2 mm radius steel sphere mounted on a pivoted brass impact hammer. The lead break signal (duration 700 μs) was much more reproducible than the impactor signal (duration 2000 μs). The most useful parameters for distinguishing the transients from the two types of source were the event duration, the rise-time and the event count.

## 2.5 Air abrasive

Hutton and Pedersen [30] have described a simple method for obtaining the relative calibration of sensor response using a small air abrasive unit to provide a broad band excitation source.

## 2.6 Helium gas jet

McBride and Hutchison [31] used the white noise energy produced by a stream of helium gas hitting a specimen surface for the measurement of the absolute signal-to-noise ratio of AE transducers. The method allows direct comparison of system sensitivities in the range 0-1 MHz, for any type of signal handling equipment. Green [32] has presented more detailed information on the technique.

## 2.7 Electric spark discharge

Hartman [33] evaluated a compact ultrasonic source for AE calibration. The device consists of a piezoelectric transient voltage source which generates a spark wave in air. The wave has high frequencies and low amplitude. Experiments to test the reproducibility and versatility were conducted. Harris [34] used spark bar calibration to predict the effect of various sensors and band-passes.

Dunegan/Endevco [35] have been using the spark impulse method for AE transducer calibration for some time. Feng [36] described the progress in spark impulse calibration techniques, with discussion of the physics and characteristics of the technique. Feng and Whittier [37] generated a convenient and reproducible AE calibration standard by initiating an electric spark above a massive (2 ton) mild-steel calibration block. The acoustic pressure wave produced by the spark (20 kV DC power supply charging a 250 pF capacitance with a 2.5 mm gap. The spark centre located 13 mm above the block with breakdown at 10kV), via thermodynamic processes, impinges on the block and is mode converted predominantly into a 100k - 1M Hz Rayleigh surface wave. Absolute calibration of a transducer requires calibration of the spark source against the NBS glass capillary source.

Egle and Brown [38] experimentally compared electric spark, piezoelectric generator and pulsed laser as AE calibration sources. The spark generating mechanism was the thermally generated pressure pulse in the air surrounding the spark. Each of the three sources was capable of generating stress waves of less than 1 μs duration.

Berry [39] proposed a modified hand-held piezoelectric torch lighter as a simple, convenient and inexpensive method of checking the sensitivity and accuracy of AE instrumentation. The spark gap can be easily adjusted to produce repeatable short-duration high-amplitude voltage spikes. The lighter is coupled to a pulser by a short length of coaxial cable.

## 2.8 Ultrasonic transducer

Dunegan and Tatro [40] used a variable frequency oscillator to drive a highly-damped 1 MHz lithium sulphate flaw detection transducer as a calibration source for sensor transducers. The calibration source had a 'fairly flat' acoustic output over a 200 kHz frequency range.

Shaw [41] established techniques for making reliable zinc sulphide on molybdenum piezoelectric films and demonstrated their use as acoustic emission devices, with a time response in the MHz range, for research and industrial applications.

Leschek [42] used a reciprocity technique for independent calibration of a transducer against a primary standard transducer. A third transducer was used to generate a gated continuous-wave sound field, which simulates the diffuse high-frequency random noise background of a nuclear reactor.

Dean and Kerridge [43] used a step waveform to shock either 2.5 MHz damped, or 1.25 MHz undamped, ultrasonic transducers to simulate the acoustic emission source. For higher source powers, the soft-tipped undamped transducer was energised with a 240 kHz interrupted continuous wave (CW) transmitter.

### *2.8.1 The reciprocity technique*

Hatano and Mori [44] developed a new method for the absolute calibration of AE transducers. A reciprocity technique in a Rayleigh wave sound field was used such that the absolute sensitivity was determined with ease and repeatability in an acoustic environment similar to that of actual structures such as pressure vessel walls.

The reciprocity principle [45] requires two transducers and an independent sound source. In addition, one of the transducers must be 'reciprocal': able to function both as transmitter and as receiver. The actual procedure is arranged such that unknown unmeasurable quantities cancel each other out and only physical constants and electrical quantities remain.

In the initial stage of the calibration, the independent transmitting transducer excites Rayleigh waves in a medium and the two other transducers are placed in the ultrasonic field in turn. The open circuit voltage, V, of each is measured. The expression for sensitivity M is M = V/pf, where pf is the (unknown) stress wave amplitude. By using the two transducers and taking the ratio of values of M, pf can be eliminated giving:

$$\frac{M_1}{M_2} = \frac{V_1 / p_f}{V_2 / p_f} = \frac{V_1}{V_2} \qquad \text{(Eq. 1)}$$

The second stage is to eliminate one of the sensitivity factors. One of the transducers is now operated as a transmitter by driving it with an electrical signal of known frequency. By considering:

- the sensitivity of the transmitter (transducer 2), with current $i_2$ flowing in it: $p/i_2$.
- the sensitivity of the receiver (transducer 1): $V_1'/p$.
- the distance between the two transducers: *d*.
- the wavelength of the ultrasonic signal, derived from the Rayleigh wave velocity: $\lambda$.
- the acoustic impedance of the medium: $Z_o$.

then the expression for the product M1 and M2 can be derived:

$$M_1 M_2 = \frac{V_1'}{i_2}\frac{2d\lambda}{Z_0} \qquad \text{(Eq. 2)}$$

and from the expressions for both the ratio and the product, the quantity M1 can be extracted:

$$M_1 = \left[\frac{V_1}{V_2}\frac{V_1'}{i_2}\frac{2d\lambda}{Z_0}\right]^{1/2} \qquad \text{(Eq. 3)}$$

The calibration can be carried out at a number of frequencies to produce a frequency response plot. Spark impulse calibration and face-to-face responses are useful as checking techniques.

Hatano *et al* [46] have described the background to the development of the Japanese Society for Non-Destructive Inspection (JSNDI) standard NDIS 2109, which deals with methods for the absolute calibration of acoustic emission transducers by the reciprocity technique.

## 2.9 Capacitive transducer

Breckenridge *et al* [18] chose a DC-biased electrostatic transducer to monitor the upper limit on the rise time of a step-function load (see Section 2.2). The output of an air-dielectric transducer used as a force transmitter should be flat with frequency (and the differentiated output should be flat with velocity), but in practice the resonance of the air gap should be considered.

Graham [24] used a capacitor microphone (600 V DC bias, 13 μm gap) as a standard for the comparison of the frequency responses of several types of AE transducer. The displacements detected by the transducers were dependent on the inverse of the square of the frequency. The output of the microphone was directly proportional to the measured displacement.

### 2.10 Pulsed laser

Egle and Brown [38] reported that the 2-J 20 ns light pulse from a Q-switched ruby laser was superior to either piezoelectric generator or electric spark simulated acoustic emission sources in its capability for generating a short-duration (150 ns) localised stress wave. The beam had an effective diameter of 1 mm unfocussed.

Holt and Goddard [47] introduced a laser pulse technique to simulate AE signals. This allowed the relevant waveguide modes to be identified and comparisons to be made between transducer-waveguide combinations.

Scruby *et al* [48] found that the thermoelastic source generated by the absorption of radiation from a Q-switched Nd-YAG laser pulse had similar characteristics to a microcrack emission source of specified orientation. The source reproduced the dipolar stress field, the time duration and the amplitude of a typical emission event. The pulsed laser was proposed as a standard simulated AE source.

Laser generated acoustic waves may be modelled in several ways. The simplest model [49], in which a small volume of material near the surface experiences a rapid thermal expansion which causes an acoustic wave, has been shown to give excellent results when compared to experimental data [50]. More complete models of the acoustic wave generation process include coupling between the propagating thermal energy and the acoustic energy [51]. The improvement of efficiencies with which laser generated acoustic waves may be coupled into test specimens has been reported [52].

### 2.11 Martensitic transformation

Brown and Liptai [53] used the martensitic phase transition in gold-47.5 atomic-percent cadmium alloy as a standard source of acoustic emissions. The results of round-robin testing of this alloy at several laboratories were presented.

### 2.12 Fracture of boron particles in aluminium

The fracture of boron particles in aluminium was proposed as a potential well-defined source of acoustic emission by Hamstad [54]. Heiple *et al* [55] measured and characterised B/2219Al during tensile deformation as a calibration source for acoustic emission.

### 2.13 Stress corrosion

Birchon *et al* [56, 57] pioneered the use of a simple aluminium block with a perpendicular cut in one surface, subjected to mechanical strain by means of a screw. When the cracked block is immersed in salt solution, the stress corrosion signals produced are very similar to those from natural cracking. It is sufficient to use just one or two drops of synthetic seawater at the tip of the machined notch.

### 2.14 Mounting condition

Higo and Inaba [58] have reviewed the general problems of acoustic emission sensors, namely:

- sensor sensitivity
- effect of mounting condition (couplant and mounting pressure)
- degradation (and it's evaluation) of the sensitivity

For dry contact transducers, the mounting pressure should be greater than 700 kPa (ASTM E650-85). Using a grease couplant, the sensitivity was found to increase with increasing mounting pressure. For the frequency range up to 2 MHz, an applied force of 300 kPa is sufficient. For detection above 4 MHz, the force should be greater than 1 MPa. A tremendous difference was found between a loose couplant condition (including bubbles) and a carefully mounted sensor. The reproducibility of the amplitude component of sensitivity is reasonably consistent for sensors carefully mounted with various couplants. However, the reproducibility of the phase component is strongly related to the couplant material. Solid or high viscosity couplants gave poor results, especially in the low frequency range.

## 3 SOURCE LOCATION PHILOSOPHIES

### 3.1 Zone location

When the geometry of a sample or structure is too complex for analysis, then only the first pulse arriving at a regular array of sensors is used (zone location). When the first transducer is excited, then a zone for the AE source region can be established from the relative positions monitored by each transducer.

### 3.2 Hit sequence

A more accurate approximation for the zone location can be obtained by using the hit sequence (Stuart's method) [59-61]. The method reduces and refines the zones defined by the single sensor zone location method, based on the order that a given event strikes a group of sensors. Each zone and sub-zone is bounded by the bisectors between sensors. The greater the number of sensors that are hit, the smaller the resulting sub-zone (Figure 1). Stuart's method is robust against inaccuracies in sensor placement, varying wave velocities and errors due to the vessel geometry.

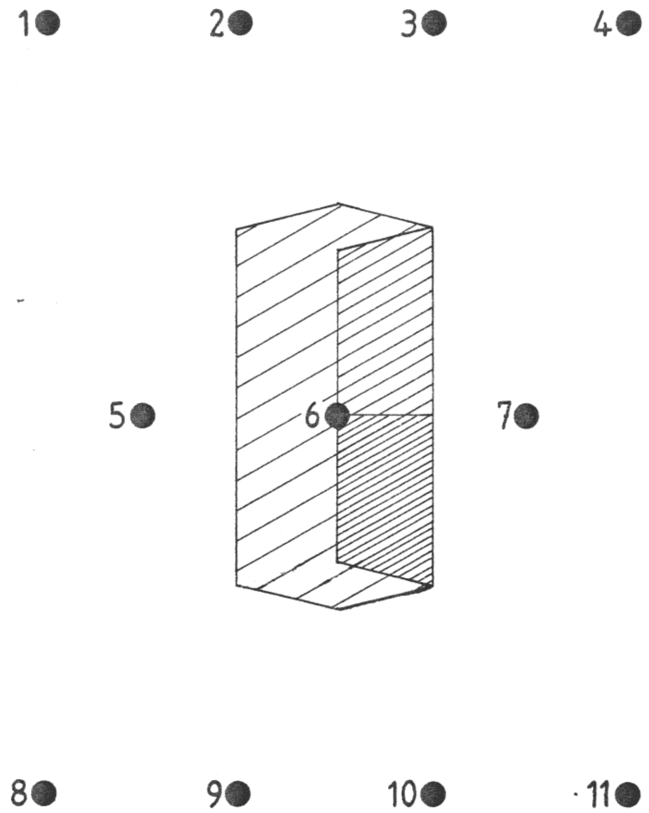


**Figure 1: Hit-sequence source location. Shading increases with number of sensors hit, hit-sequence was 6, 7, 10 (after T J Fowler, reference 61).**

A recent refinement of Stuart's method uses energy based severity analysis to group adjacent sensor hits into specific events. This is particularly useful when a large number of events occur in a short time period, typical of bursts of emissions, low attenuation structures and noisy environments.

### 3.3 Triangulation

#### *3.3.1 Time-of-arrival location*

Time of arrival location uses the relative arrival times of the stress wave at a set of transducers. When the stress wave travels through the material at a known constant velocity, and if enough sensors are hit, then triangulation calculations can be carried out.

Triangulation can work well on flat plates in a laboratory, but is rarely ideal on actual vessels under field conditions. Data from field tests on metal vessels [62] have shown that the number of locatable events may be in the range 0-20% of the total number of hits. The causes include stress wave attenuation, vessel geometry, distortion at discontinuities (especially welds), shielding by nozzles and pipework and wave-mode conversions. A major problem is the rejection of data which fails to meet predetermined locatability criteria. Contemporary (1984) practice was to record all data with real time zone location and subsequently conduct more accurate source location during post-test analysis.

A second problem can occur with systems which shut-down ("lock-out") the first-hit transducer (and often sensors in adjacent sub-arrays) until adjacent transducers have received a hit from the same event or until a predetermined time has elapsed. During the dead period all information at locked transducers is ignored. To avoid this some systems do not classify transducers into specific sub-arrays, but record all events with an arrival time and use the first three hits to triangulate a source location.

Triangulation is based on assumptions about geometry, accuracy of sensor placement, constancy of wavespeed and accurate measurement of relative arrival times. Small deviations in these parameters can cause major errors in the calculated source location. Background noise, multiple sources, multiple paths, reverberations, wave dispersion and changes in wave mode/frequency further frustrate accurate location.

### *3.3.2 Measurement of arrival times*

In some industrial applications of AE, such as pressure vessel testing, it is important to locate the presence of cracks or defects. In using triangulation techniques for source location, the relative arrival times of an emission signal at the transducers are used. It is therefore important to take into consideration a number of potential problems which may be encountered:

- Relative arrival times need to be measured with sufficient accuracy
- The solid specimen can propagate the emission signal in a number of modes (compression, shear, plate, and surface waves), each with a characteristic velocity
- Incident and reflected waves at a boundary will interact, resulting in pulse distortion and possibly mode conversion.
- The signal can be attenuated by a number of mechanisms (dislocation damping, internal friction, deformation hysteresis and micro-creep). Viscoelastic damping is proportional to the square of the frequency and hence higher frequencies will be more rapidly attenuated.
- At frequencies greater than 100 kHz, the loss from scattering at interior grain boundaries can become more significant than the aforementioned attenuation mechanisms. At inclined boundaries, mode conversion between compression and shear waves can occur.
- If the specimen material is dispersive (sound velocity changes with wavelength), then the component frequencies of the pulse become separated in phase, leading to distortion of the original waveform. Most bulk materials are non-dispersive, except in the neighbourhood of phase transitions or order-disorder phenomena.
- In bodies with limited dimensions, the conditions near to boundaries can render the system shape-dispersive.
- In complex shapes when there is no direct source-transducer path, "shadowing" effects are possible. Ideally transducer positions should be selected to minimise shadowing effects.
- Background signals from mechanical or hydraulic noise are also received by the sensors. The acoustic emission of a crack growth event is impulsive with a characteristically sharp rise time. However, even after pulse broadening during propagation the defect signal retains a sharp rise time. This can be useful in deciding if a signal originates from a defect or from background noise.

The leading edge of the received pulse is often used to define the time of arrival at the sensor. It is therefore desirable to know that the specific propagation mode of the disturbance has a definite velocity, at various distances in the range of interest, to confirm that the leading edge has the frequency content expected.

For a source-transducer distance of 1 m, the total error has been estimated to be about 20 μs, corresponding to a distance of just over 10 mm [63]. If it is possible to perform the timing at the arrival of the peak pulse height, instead of the leading edge, some of the error can be eliminated.

Stephens and Pollock [64] indicated the information present in waveforms and spectra of AE signals. The effects of multiple reflections and of resonances were discussed. It was proposed that an AE source should be modelled as a pulse, rather than as an oscillatory, function. A theoretical analysis of longitudinal modes in the sample was presented, and it was observed that emission spectra are influenced by structural resonances.

Experiments by Fowler and Papadakis [65] indicated that the first arrival of emission energy was at the velocity of the first longitudinal mode of the plate, confirming the work by Stephens and Pollock. A strong signal at the velocity of the first flexural mode follows the longitudinal signal. The flexural signal may be much stronger than the longitudinal mode.

Hsu and Jeong [66] studied the ultrasonic (4 MHz and 8 MHz) velocity change and dispersion due to porosity in composite laminates. In both quasi-isotropic graphite/epoxy and woven graphite/polyimide, correlations were observed between decreasing velocity and increasing porosity. The velocity in composites with voids was found to be more dispersive than that in void-free composites.

As the measurement of $\Delta t$ becomes more ambiguous, the velocity as a function of frequency should be measured using a phase spectroscopic technique [67]. Li and Thompson [68] have modelled the pulse distortion and phase shift for pulse propagation in a dispersive medium, and studied the Gaussian shaped spatial envelope.

Wu and Ho [69] studied the energy and phase velocities in a 36-layer unidirectional T300 carbon fibre composite. The deviation of the respective propagation directions was found to be as large as 60 degrees. The measured energy velocities were transformed to phase velocities by employing a numerical scheme.

### 3.4 Iteration

Sleptsov and Zhirkov [70] have proposed a system for the localisation of acoustic emission sources by means of successive approximation from three minimum time delays using integer calculation on a personal computer. The proposed algorithm is claimed to reduce loss of useful information, increase location accuracy and increase the rate of initial data processing when compared to the IV Kurchatov Institute of Atomic Energy asymptot method (quoted but not referenced in the paper).

### 3.5 Learning algorithms

Artificial sources may be used to obtain delta-time values, which are stored in computer memory and subsequently used for comparitive purposes in adaptive learning methods (Figure 2). These systems can be used with any array configuration, and are particularly useful for irregular geometries (dished ends, knuckle radii, etc) when triangulation methods may be inaccurate.

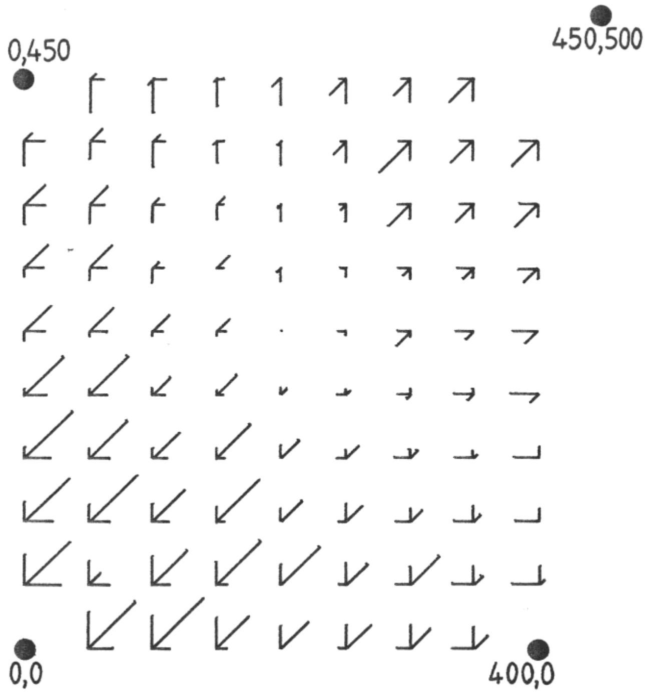


**Figure 2: Relative arrival times measured on a woven fibreglass panel, dimensions in millimetres. The lengths of the three lines are each proportional to the delta-time between the respective transducer pair (horizontal, vertical or diagonal). (after Ibitolu and Summerscales, reference 200)**

Grabec and Sachse [71] have described a novel approach, based on a simulated system which resembles the structure of an intelligent neural network. A systematic series of simulated sources were presented to the system. The adapted system could then recover the characteristics of an unknown source from the detected signals. It could also synthesize AE signals from the source properties without using any elastodynamic theory.

### 3.6 Correlation functions

If two omnidirectional point receivers are located at points $X_1$ and $X_2$ in a homogeneous noise field and the outputs of each receiver are proportional to the pressure at each point and are added, squared and averaged over time, then we obtain [72]:

$$< e^2 >_2 = 2 < e^2 >_1 \left[1 + \rho\left(X_1, X_2, \tau_{12}\right)\right] \qquad \text{(Eq. 4)}$$

where $<e^2>_1$ and $<e^2>_2$ are the mean square outputs of one receiver alone and of two receivers, respectively and $\rho(...)$ is the normalised spatial correlation function of the noise pressure at the two points with delay time $\{\tau_{12}\}$. The spatial-correlation functions for different types of noise field can be obtained by calculating the two $<e^2>$ values and using Equation 4.

Cron and Sherman [73] used cross correlation techniques for linear flaw location and showed that the optimum spacing in an array depends strongly on the characteristics of the noise field in which the array is used. Specific directionality functions (SDFs) were considered for the omnidirectional case, $g(\alpha) = 1$, where the surface noise source is a directional radiator with amplitude directionality given by the function: $g(\alpha)$. The special cases where the receivers are parallel and perpendicular to the surface, $g(\alpha) = cos\ (\alpha)$, were also considered.

Grabec [74] used a correlation function measurement to estimate a characteristic time delay between the continuous AE signals (of corrosion processes) from two AE transducers and hence localise the source. This estimation is only possible if the emission is uncorrelated in time and originates from a small area of a large system without reflections. A mathematical model for the description of emission, propagation and detection of ultrasound under such restricted conditions was presented. The applicability of the model to experiment was demonstrated with real and simulated AE sources in an aluminium bar. The resonances in the detection system introduced difficulties although these could be overcome by increased damping of the transducers (albeit with reduced sensitivity). Ideally each transducer excitation should be reduced to a single pulse.

### 3.7 Radiogoniometric principles

A new approach to AE source location has been derived from the principle of radiogoniometry [75, 76]. An active localisation was used in which the solution was derived from the phase delay between responses at a close group of transducers. The signals add constructively only for the direction or point determined. Holler *et al* [77] have described a double concentric circular array with 6 transducers on an outer 100 mm diameter locus and six transducers at the intermediate 30 degree positions on the inner 60 mm diameter.

### 3.8 System accuracy

Nankivell [78, 79] has described the application of a computer program written to assess the effects of uncertainties (AE pulse propagation speed and measurement errors in arrival timings) and errors in source location by time-of-flight methods. A 1000 mm square array of point sensors on a 100 mm grid was considered. Arrival time differences were computed for AE sources at all unoccupied grid points. Figure 3 shows the 'REACH' (distance from the centre of the array to the location error boundary) for a square array, and how inaccessible regions behind the sensors can be eliminated by a 'double square' array of eight sensors (equally spaced around a circle of 707 mm radius). Three routes to improved source location are recommended:

- that each sensor is triggered by the same wave propagation mode,
- that timing difference accuracy is better than 100 μs, and
- that the actual propagation distance should be determined, taking account of variations in propagation speed with changes in effective cross-section.

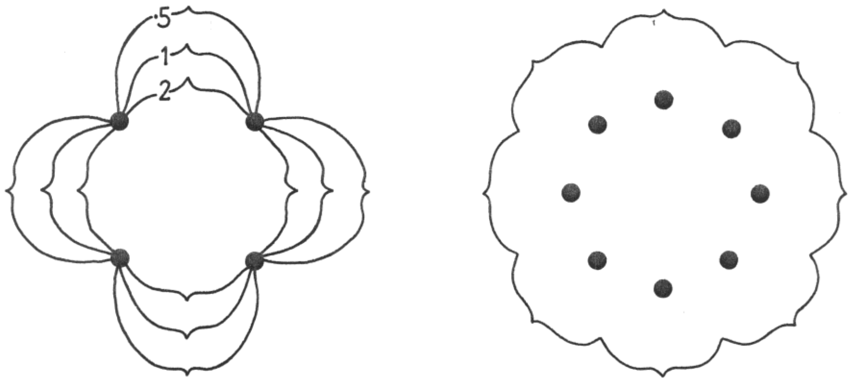


**Figure 3: Left: 10-millimetre location error boundaries for 0.5, 1 and 2 microsecond timing errors**
**Right: 10-millimetre location error boundary for a 0.5 microsecond timing error**
**Both arrays use a 1000 mm square sensor set, right-hand set uses a double array**
**(after Nankivell, reference 79).**

### 3.9 Standard procedures

The European Working Group on Acoustic Emission (EWGAE) has produced a code of practice [80] which includes systems, equipment and personnel for carrying out defect location by acoustic emission. The code sets out the information required prior to testing, methods for carrying out calibration, verification and examination, details of data analysis and recording, and reporting of results and conclusions. The code outlines precautions to be taken to minimise location errors, and to recognise regions of good and poor source location accuracy. The test preparation draws attention to the importance of knowing:

- full geometric and lay-out details of the vessel
- materials specification and heat treatment history
- locations of known defects, and
- results of previous tests

The ASTM Standard E569 [81] dedicates just one paragraph to source location accuracy.

## 4 SOURCE LOCATION IN ISOTROPIC MATERIALS

The initial work on acoustic emission source location (AESL) was done in the 1960's by Allen Green *et al* at Aerojet General for the computer-based SWAT system. Dwight Parry (then at Phillips Petroleum) demonstrated his source location work using a computer to solve for delta-times at the first Acoustic Emission Working Group meeting during February 1968 at Idaho Falls [82]. The majority of systems use the signal arrival times at different transducers. Where practicable, the arrival of different modes of propagation can be exploited to increase confidence in the location of the AE event.

### 4.1 Linear source location

If an acoustic emission source lies on a straight line between two transducers, the arrival time will differ at each transducer unless the source is exactly half-way between the transducers. The sum of the arrival times ($T_a$ = time from source to transducer A, $T_b$ = time from source to transducer B, V = velocity of the wave, and x = distance of source from mid-point of array) will be the time to travel between the sensors, characteristic of the mode of propagation in the material. The distance of the source from the mid-point can be calculated from:

$$x = V\,(T_a - T_b)\,/\,2 \qquad \text{(Eq. 5)}$$

where $(T_a - T_b)$ is the difference in the arrival times measured by an electronic timer. If x is negative, then the source is between the midpoint and transducer A.

Vasil'ev and Maslov [83] have described a graphical system for the determination of linear (or ring) source location on an object with multiple equally spaced transducers. If channel *j* receives the first pulse, then subsequent transducers will be hit in the sequence:

*j, j-/+1, j±1, j-/+2, j±2, ....*

Where plus and minus are in opposite directions from the source. In the minus direction transducer numbers will decrease to 1, in the plus direction numbers will increase to *n* (the total number of transducers). The timing diagram (Figure 4) can be constructed and as all inter-transducer distances are equivalent, all differences in arrival times are the same in both directions. Calculations were presented for estimation of the number of receiving channels required as a function of detection reliability, the accuracy of the source co-ordinates and the noise environment.

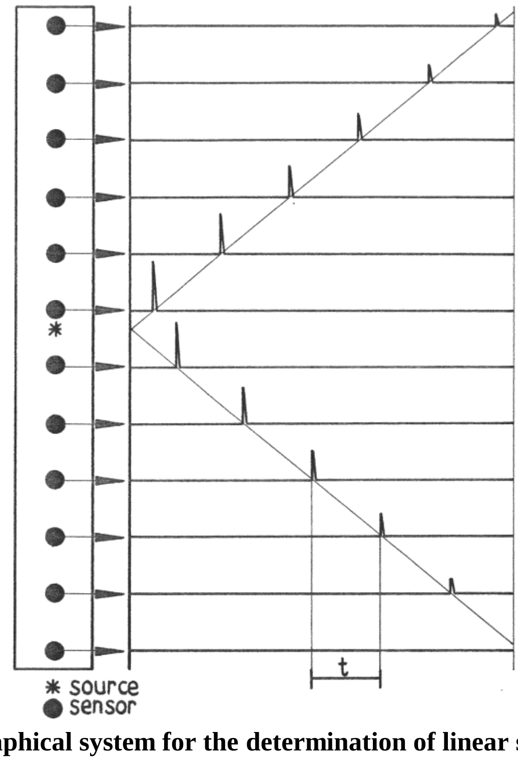


**Figure 4: Graphical system for the determination of linear source location (after Vasil'ev and Maslov, reference 83).**

Maslov and Vasil'ev [84] considered the errors associated with incorrect arrival time differences and incorrect velocity values for three linear array configurations:

- two transducers
- three equally-spaced transducers
- two pairs of closely spaced transducers at extreme ends of the line

The conventional linear location using two transducers is characterised by a transit-time error and an appreciable velocity error. Three transducers permit a reduction (and in some cases elimination) of the velocity error, albeit with a slight increase in transit time error. The four transducer scheme almost completely eliminates velocity errors and thus affords greatest accuracy (although time-transit errors are further slightly increased).

Moeller *et al* [85] developed a technique to determine crack front length and location by sorting AE data from two sensors in the Fourier domain. For structural ceramics (alumina or silicon carbide), good correlation was seen between actual crack lengths (measured with dye penetrant after each cycle of 'double torsion' testing) and crack lengths determined by acoustic emission.

Grabec and Sachse [86] have reported a simulation demonstration of a simple intelligent system for use in linear and areal source location. This could distinguish the ball size in drop impact source simulation.

Hardy *et al* [87] studied the use of mechanical waveguides and acoustic antennae embedded in geological materials. The monitoring capability of acoustic emission/micro-seismic (AE/MS) systems in a deteriorated rock mass can be enhanced by the use of embedded mechanical waveguides. Conventional waveguides are unsuitable for source location since the actual point of impact of the stress wave on the waveguide is not known. A "dual-transducer waveguide" with a transducer on each end allowed linear source location of underground AE/MS sources within the rock mass.

### 4.2 Areal source location on flat surfaces

Hoff [88] used two concentric four transducer arrays to scan the whole area of a 0.91 m diameter diaphragm, or six possible combinations of four transducers to obtain higher resolution. Pulse excited ultrasonic transducers and spark gap were used as calibration sources. Two separate timing circuits were used to measure relative arrival times at opposing pairs of transducers. The delay time in each circuit was proportional to the magnitude of the combined circuit voltage and the sign indicated which transducer was excited first. A computerised system using geometrically resolved statistical enhancement techniques was used to reject insignificant signals.

Various algorithms exist to accommodate mathematically simple structures. These may be combined to cover more complex geometries. An algorithm for Acoustic Emission Source Location (AESL) using circular wavefronts on a flat isotropic plate has been presented by Tobias [90, 91]. This was developed by the CEGB Berkeley Nuclear Board for the field testing of pressure vessels as the ACEMAN (ACoustic EMission ANalysis) system [92, 93]. The system uses up to 12 surface wave sensors operating on a 165 kHz band centre. Timing can be either at the signal peak (for simple structures) or at a leading edge (with more complex arrays). The sound from a defect in steel travels at approximately 3000 m/s (Rayleigh waves). The relative arrival times at each pair of transducers determines a difference in the distance of the source from each of the transducers. Each transducer pair thus predicts an hyperbola on which the source lies. The intersection of any two hyperbolae is the required source location. A minimum of three transducers are therefore required, but a fourth transducer is usually employed to resolve ambiguities or to confirm the calculated position.

A similar exact solution approach (Apollonian circles) was described by Bell [94] using a centred equilateral-triangle four-transducer array to locate sources within a larger regular hexagonal area (hexagon edge = 2.25 x triangle edge).

Chretien and Perennes [95] examined several solutions to the AESL problem on surfaces: graphical, analytical and numerical methods. They concluded that the square pattern formed by four transducers with a fifth central transducer offered the best precision on the largest area.

Fontana *et al* [96] have also described a similar analytical algorithm for AESL on pressure vessels using intersections of hyperbolae defined by arrival time differences. It was assumed that the detected wave would usually be in the transverse mode. For cylindrical and other surfaces the solution was consigned to "apposite numerical methods on a digital calculator" (with at least 8K memory) with source accuracy limited to the areola contained between the two branches of the hyperbolae with coincident foci. An alternative mode of operation was proposed such that source locations were only calculated at positions with concentrated active sources, using the averages of multiple time differences from that region.

Fontana *et al* [97] at CISE in Italy developed an AESL system for thin-walled pressure vessels. Although the longitudinal wave is faster than other modes of propagation, the fraction of the total burst energy converted to this mode is small and decreases with distance from the source. Longitudinal waves thus have small amplitudes and high attenuation. The system utilised an (800 mm edge) equilateral triangular array of 200 kHz resonant PZT-5A transducers, and a delta-time hyperbolic triangulation algorithm. The signal from a piezoelectric transducer was fed through a metallic cone to obtain a very small contact area for calibration of the array at 48 points. Within the array the location error was less than 20 mm. The location error loci for timing and wave velocity errors are shown in Figure 5, where T1, T2 and T3 are the transducer positions. Golinelli [98] has described the microcomputer used in the CISE system.

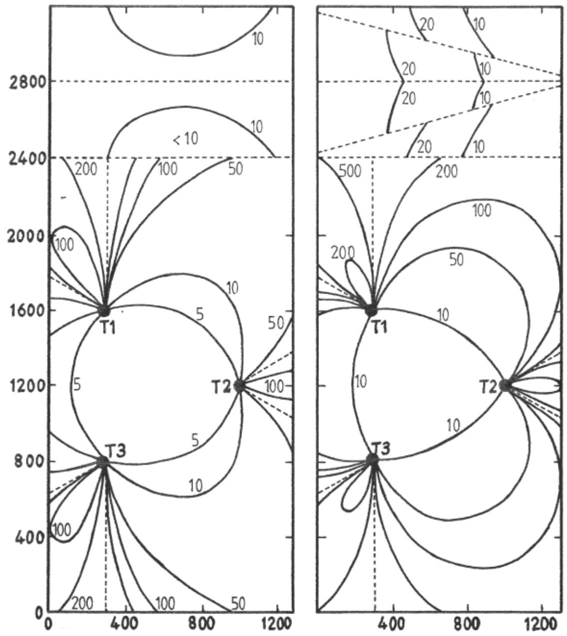


**Figure 5: Location error loci for a 1 us delta-time error (left) or for a 100 m/s propagation velocity error (right). (after Fontana *et al*, reference 97).**

Onoe *et al* [99] developed (simultaneously with the UK, US and Italian systems above) a multi-channel on-line AESL system using the intersection of pairs of hyperbolae. A (square) diamond array with transducers on each of the positive and negative axes was used to locate concentrations of acoustic emissions during a fatigue test of a model nuclear reactor vessel.

Hatano [100] proposed the use of face-centred transducer arrays and a hard-wired logic selector (Figure 6) for AESL, eliminating the need for a computer. The logic selector chooses two pairs of detectors dependent on which transducer is activated first, and applies the pulse in each channel to two time-difference counters. When the source is at the boundary of the localisation range, the error is about 1.5% of the lattice period.

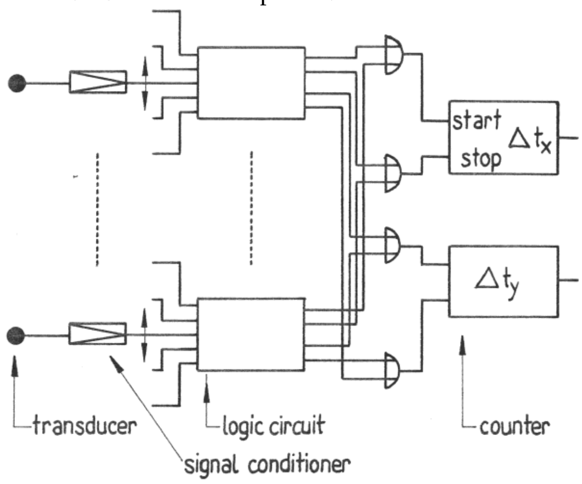


**Figure 6: Block diagram of a multi-channel location system. (after Hatano *et al*, reference 100).**

Anisimov *et al* [101, 102] have presented a method for determining the source of discrete acoustic emission signals from the time intervals between four transducers. The time interval was referenced to the transducer at which the last signal was received. The x- and y- co-ordinates of the source were calculated from:

$$x = k\,(\Delta T_1 + \Delta T_2 + \Delta T_3 - \Delta T_4) \qquad \text{(Eq. 6a)}$$
$$y = k\,(\Delta T_1 + \Delta T_2 - \Delta T_3 - \Delta T_4) \qquad \text{(Eq. 6b)}$$

where $\Delta T$ is a time interval and $k$ is a proportionality factor ($k$ is reported to be $c/(2\sqrt{2})$, where $c$ is the speed of propagation of the signal [103]).

Vainberg and Dekhtyar' [104] produced a comparitively simple hard-wired device to determine the AE source co-ordinates without a computer, by using the above approach. In monitoring a growing fatigue crack in a camshaft, co-ordinates were determined within 12% error limits.

Anisimov [103] has studied those situations where wave propagation rates are different to those set in the device, or different waves are recorded at different sensors. The selection of working points on the Lamb wave dispersion curves (such that the ratio of values of group speeds of zero modes exceeds 2.1) greatly simplifies the unambiguous determination of the co-ordinates. A further option would be to increase the number of groups of sensors.

Barsky and Hsu [105] constructed a simple electronic acoustic emission system to utilise the above method. Arrival time differences at four transducers on a square array were used to provide zone location indicated by a 16x16 grid of light emitting diodes. The relative intensity of the LED's corresponds to the number of events in the particular region.

Khol'kin [106] examined amplitude-spatial diagrams for AE signal sources and showed that when the transducers were too widely spaced, there were dead zones for the location and for the detection of useful signals. Formulae were derived for calculation of the maximal distances permitted between transducers for the inspection of one- and two-dimensional objects, with relationships for finding the probability of undetectable AE signals.

Obata [107] used AE to monitor fatigue tests on thick compact tension (TCT) specimens of stainless steel or aluminium alloy. Two-dimensional source location in the plane of the advancing crack was determined using four surface mounted transducers on a 50 mm square array. The source location error towards the centre of the array was 1 mm, but at the corners could be as high as 8 mm.

## 4.3 Areal source location on curved surfaces

### *4.3.1 Source location algorithms*

The Commissariat a l'Energie Atomique (CEA) derived a suitable algorithm for the location of sources on a spherical surface. Such a method can obviously be applied to source location on a plane surface by increasing the radius of the sphere to infinity. In a consideration of the CEA system [6], Drouillard [2] indicates that the "square pattern formed by five sensors with a central sensor leads to the best precision on a large area", while Bassim and Houssny-Emam [108] suggest that "arrays of equilateral triangles constitute the most favourable configuration".

Podgornyi and Guz' [109] presented a technique for the detection of defect co-ordinates on the surface of spherical parts of constant radius. The surface was divided into spherical triangles with sensors located on the intersections of the geodesic arcs of the great circles.

Asty [110] has presented the mathematical solutions for both spherical and plane surfaces. The equations can be solved by computer calculation, although great care must be taken to avoid singularities, and certain coefficients may undergo very large variations which require a high degree of precision in numerical values.

Anisimov has extended his method for AESL on flat surfaces to large conical surfaces [111], developable surfaces [112], parts of spherical surfaces [113] and has suggested that transition surfaces may be handled with preliminary calibration [114].

Nakasa [115] has presented general calculation methods for AESL on 3-D structural components (flat or curved planes, cylinders, cones, torus and spheres). A rotational graphic display was demonstrated to be an effective mode of presentation. Typical results of numerical experiments on a personal computer indicate that good location accuracy was obtained. The system could also be used to optimise the transducer configuration and to evaluate location data after tests.

An acoustic emission point source located on a thin spherical shell generates sound waves which propagate along the great circles passing through the point. Burenko and Whittaker [116] used four sensors placed at 90° from each other on the surface of the spherical shell in two normal planes. The four-channel time-differences were converted to the spherical co-ordinates of the point source. A graphic display [117] has been designed to alternately display two hemispheres. Azimuthal Equidistant Projection was used.

Yoon, Kim and Kwon [118] have proposed a simplified AESL algorithm using the circumferential wave paths on cylindrical vessels. The time differences (not between each sensor but) between each path were considered. The concept of virtual sensors was introduced to allow the use of a single sensor, but problems of multiple predictions due to vessel symmetry need to be solved. A dual sensor configuration was used on a six-metre long 1.05 m diameter cylindrical pressure vessel with pencil break calibration. Good agreement between calibration position and calculated source location was obtained within the bounds of experimental error, with one exception due to a sensor dead zone. However, the calibration positions were on the two orthogonal axes parallel to the cylinder axis and bisecting the transducer x- and y- co-ordinates: the positions where the lowest errors would be expected.

The problems of multiple predictions due to symmetry have been resolved [119] by the use of a dual sensor configuration. The dead lines can be covered by conventional planar location, or by employing a supplementary set of dual sensors. The hemispherical closure sections in cylindrical vessels have to be monitored by a conventional planar location method.

### 4.3.2 Location systems and applications

Birchon *et al* [56] commissioned a mobile 20-sensor automatic Defect Location System (DLS) for pressure vessel testing in 1972. Four sensors, and three time differences, were used to accurately locate the source of the emission. The direct calibration (algorithm not specified) produced two solutions, requiring the data from the fourth transducer to determine the correct source. The solution was only accepted if the time difference between the first and fourth transducers from the calculated source were within a preprogrammed error bound for the third time difference.

Parry [120] described a portable location and analysis system known as ACOUST, which was operated by the Exxon Corporation. Fault diagnosis was carried out with reference to accumulated energy count and to time analysis of the received signals. Output from the system was presented as a digital map with the severity of the defects represented by the numbers zero to nine.

Watanabe *et al* [121] have reported the acoustic emission inspection of two water-pressure fracture tests of welding defects in 1.5 m diameter 4.84 m long steel pressure vessels. The 32-channel Nippon Steel AE inspection system (NIAS 32) was used. Source location was achieved by measuring the relative arrival times of signals exceeding a 0.5 mV peak-peak threshold, on the sensor output, at more than three adjacent sensors. The pulse height of the first signal received was used to estimate the emission energy. Clusters of located signals were observed for some of the NDIS class-4 (major) defects.

Horak and Weyhreter [122] reported the design and testing of a real-time system which integrated known noise discrimination techniques with computerised source location equipment. The spatial noise discrimination involved concepts of rise-time, master-slave and coincidence detection to eliminate undesired signals.

Kuehnicke *et al* [123] have proposed that the signals from the various sensors can be switched to a single summation channel using simple gate circuits. The electronics required can hence be greatly reduced if the sensor hit time is recorded but the arrival sequence is omitted. However it is necessary to measure at least three time-lags, rather than the usual two in multi-channel systems. When a sensor hit is detected, only the first few microseconds are fed to the summation channel. Resolution capability is not reported.

Crostack and Engelhardt [124] have proposed a receiver consisting of multiple transducer elements. Because the transducer array elements are small and hence can be located in close physical proximity, there are no essential differences in the received signal amplitudes at each element, provided that sensitivities are correctly adjusted. The use of such a single receiver assumes that each element receives the same sound wave propagation mode and velocity as the signal is essentially from a single direction. Two elements permit the determination of the direction of the source for a known sound velocity, or the same result may be obtained by simultaneously eliminating the sound velocity. While the source to receiver can be determined with good resolution, the evaluation of distance is restricted to certain ranges. Sources at longer distances may be located by intersection of directions for two different receivers. This latter approach yields good site results, except where the source is on the direct line between the receivers.

Fowler *et al* [125] have described the MONPAC acoustic emission based system for evaluating the structural integrity of metal vessels and pipelines. The system comprises a technology package (reports of laboratory and field tests with case histories), a comprehensive test procedure, an instrument and a User Group. The test procedure first identifies and removes "non-genuine" emissions, then compares the remaining "genuine" emissions against predefined MONPAC evaluation criteria. Improved post-test analysis methods, including correlation plots, standard filters and intensity analysis (with MARSE: measured area under rectified signal envelope, Figure 7) have led to a more accurate assessment of the nature, severity and location of defects. The post-test intensity analysis is referred to as a Zone Intensity Processor (ZIP). The technique compares the change in MARSE throughout the test (historic index) with the events having large MARSE values (severity). In addition to ZIP, intensity values and positions are shown on a graphical representation of the vessel.

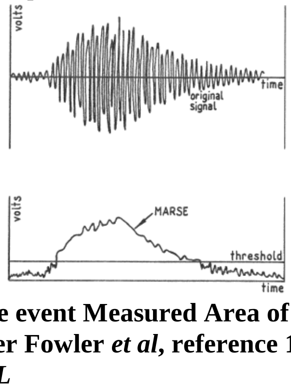


**Figure 7: Schematic repesentation of the event Measured Area of the Rectified Signal Envelope (MARSE) (after Fowler *et al*, reference 125).**

### 4.3.3 Commercial systems suitable for AESL

Physical Acoustics Limited (Cambridge UK) [126] and Physical Acoustics Corporation (Princeton NJ) introduced an eight-channel LOCation ANalyser (LOCAN) for acoustic emission source location in 1986. The system is derived from the microprocessor-based 3000-series and utilises the single board Independent Channel Controllers (ICC) from the SPARTAN distributed parallel processing AE system architecture. Optimum performance is achieved using innovative Spatial Filtering. Optional guard channels make LOCAN suitable for small specimen work, production weld monitoring and quality inspection and testing. The initial system could acquire more than 1500 hits/second, with upgrades to 10000 hits/second in prospect. In 1988, the system was extended up to 14 channels and integrated with an MS-DOS operating system and an Intel 16-bit processor as the LOCAN AT [127]. The application software was programmed in "C" for modularity and portability.

Speedtronics Limited (Huntingdon UK) [128] offered a range of products with multi-channel capability suitable for AESL. These include:

- the AECL (Huntingdon UK) 2100.M modular system,
- the AET (Sacramento CA) 5000B 2-8 channel analyser,
- the Hartford Steam Boiler (Sacramento CA) Composite Tester, and
- the AVT (Stockport UK) Vulcan V8SM Structural Monitor.

The AET system [129], based on a North Star Advantage computer, offers linear, zone calibration, first-hit, spherical, three-dimensional and delta-time real-time source location. The interface can handle more than 3000 hits/second, with recording to hard disc at 250 events/second.

Stresswave Technology Limited (Wirksworth UK) [130] have introduced an intuitive sensor system using neural networks from Rolls-Royce and Associates Limited (Derby UK). The system senses high-frequency stress waves, and draws upon past experience or training, together with advanced pattern recognition and classification software to correlate particular stress wave patterns to their causes. A high-frequency (100-500 kHz) sensor [131, 132] includes the transducer, filters, amplifiers and processor to provide a high level of enveloped output (reduced from radio frequency to audio frequency) which can drive cables up to 100 metres long. The sensor package measures only 32 by 32 mm and is housed in a stainless steel shell for electromagnetic shielding and mechanical protection. The output can be fed directly to an appropriate analogue input port of a personal computer, eliminating the need for conventional acoustic emission instrumentation. At 500 kHz, the signal on GRP was attenuated from 0 dB at 50 mm to -22dB at 250 mm. The sensor would appear to be suitable for first hit, zone location and relative response (including MARSE) source location.

### 4.4 Volume source location

Anisimov [133] has further extended the method for AESL on flat surfaces to the three-dimensional location of discrete acoustic emission signals in monolithic isotropic test-pieces, using eight sensors placed at the corners of a cube. For situations where a cube-array is impractical, scaling factors may be introduced for sensors placed on a rectangular parallelepiped, although the error increases with deviation from the cube. A preferred method for monitoring a rectangular prism would be to use 16 transducers to form a contiguous array of three cubes. The design of the apparatus [134] is analogous to that for 2-D AESL, and determination of the co-ordinates is instantaneous with reception of the signal at the last channel.

Maslov and Vasil'ev [135] considered that the Anisimov approach had a number of essential drawbacks: the large number of sensors, the need for two-sided access and the errors due to the linear approximation of the hyperbolic functions. A rectangular or square transducer array precludes the determination of source depth information on a straight line through the centre of the rectangle and perpendicular to the surface. They adopted an array with sensors at the centre and corners of an equilateral triangle, and a cylindrical co-ordinate system. The possibility to accurately determine all three co-ordinates of an AE source was claimed.

Scruby *et al* [136] have described a calibrated 6-channel recording system for the detection, location and characterisation of AE events. The 3-D force dipole representation of each event was deduced from the arrival strengths by inversion of the Green's tensor. In a simulation study, an error of 0.05 μs (equivalent to the digitisation increment) in one arrival time caused a maximum error of 0.3 mm in any coordinate for the six-channel system and 0.5 mm for a four-channel tetrahedral array. Additional channels are thus useful for improved location accuracy. In practice, the maximum difference between co-ordinates located by four- or six-channel systems was 0.3 mm.

Kim *et al* [137] used a six-transducer digitised-wave acoustic emission system to monitor the nucleation of microcracks or breaking of inclusions in three titanium alloys, two steels and alumina ceramics. Three-dimensional location was established by measuring the time-differences for the initial longitudinal waves between two independent transducers and using a non-linear least squares method (Newton-Gauss repetition equation). The six-channel system used 500 kHz resonant transducers to monitor 25 mm thick compact tension (TCT) fracture toughness specimens.
Kishi and Enoki [138] have extended these experimental procedures for three-dimensional location using a dynamic Green's function obtained from the finite difference method. The source moment tensor was calculated by time domain deconvolution. The system has been used to monitor titanium alloy [138] or silicon nitride [139] TCT specimens.

Nagano *et al* [140] have developed an automatic AESL algorithm for downhole triaxial measurement of AE from sub-surface cracks. P-wave arrival time was determined by analysis of the cross-correlation coefficient between three components using a 'composite energy comparison method (CECM)'. The algorithm uses the triaxial hodogram method, rather than the travel-time difference method. The system can locate an AE source as accurately as 'human analysis' provided that the signal/noise ratio (S/N) of the AE signal is greater than 4 dB. A significant error is produced when the S/N is below 4 dB [141]. A concept of AESL confidence evaluation [142] has been presented in order to realise a more reliable automatic system.

Getting *et al* [143] have reported studies on the accuracy of source location in anisotropic Westerly granite. Three techniques were examined:

- an isotropic fixed velocity model
- the observed anisotropic, stress-dependent velocity field, and
- transducer size corrections.

The determination of the velocity field throughout deformation was critical to accurate location. The effective transducer position was also important.

Labuz *et al* [144] found that the measured P-wave velocities in charcoal granite had a large influence on the estimated source location. A 10% variation of the velocities in the three orthogonal directions resulted in a location error of 10 mm or greater for almost half the test points (against an accuracy of ± 5 mm with correct values for a trapezoidal array contained in a 200 mm square area).

Maxwell *et al* [145] have proposed a method to simultaneously determine source locations and passively image the velocity structure of a deformed sample. The method uses arrival time data measured from recordings of induced (geological) acoustic emissions. The velocity structure image was sensitive to the state of stress in the sample and could be used to map spatial variations in stress induced changes. Sequential passive imaging should prove to be a powerful tool for imaging evolving in-situ stress fields.

Ge and Hardy [146] considered the effect of 3-D array geometry on source location accuracy to be very complicated. In terms of hyperbolic field theory, the effect can be resolved into two basic elements: geometrical spreading and direction control. Thus a theoretical basis is provided on which to develop a strategy for diagnosis of the major weakness of a proposed array. The changes necessary to achieve an optimum array geometry can then be objectively made, by use of a 'control transducer pairs' concept. It is then possible to use a relatively shallow transducer array to monitor a deep area with balanced accuracy in all directions.

The success of source location is partially dependent on the choice of algorithm used. The Newton Least Squares (NLS) algorithm is one method that has been used [147]. In applications where the acoustic wave has been attenuated or is buried in the background noise it is difficult to obtain accurate arrival times, and such errors often lead to failure of the NLS algorithm to converge to a localisation solution. Simplex optimisation is a well-known method for sequential optimisation of multivariate experimental systems, first described by Nedler and Mead [148].

Collins and Belchamber [149] compared the Composite Modified Simplex (CMS) algorithm [150], which more efficiently converges to an optimum, against NLS. Each algorithm was allowed 100 iterations. Figure 8 illustrates the effect of arrival time error on the accuracy of simulated source locations, where varying degrees of measurement error were introduced by adding a random number to the calculated arrival times. For real 3-D data (expanding grout filling a hole in a concrete beam), approximately two-thirds of the NLS data failed to converge to a solution. The simplex method presented a location in every case where at least five (of eight) transducers detected acoustic emission. When the P-wave velocity is precisely known, then NLS provides superior results. The Simplex method performs better for unknown velocities and high measurement errors.

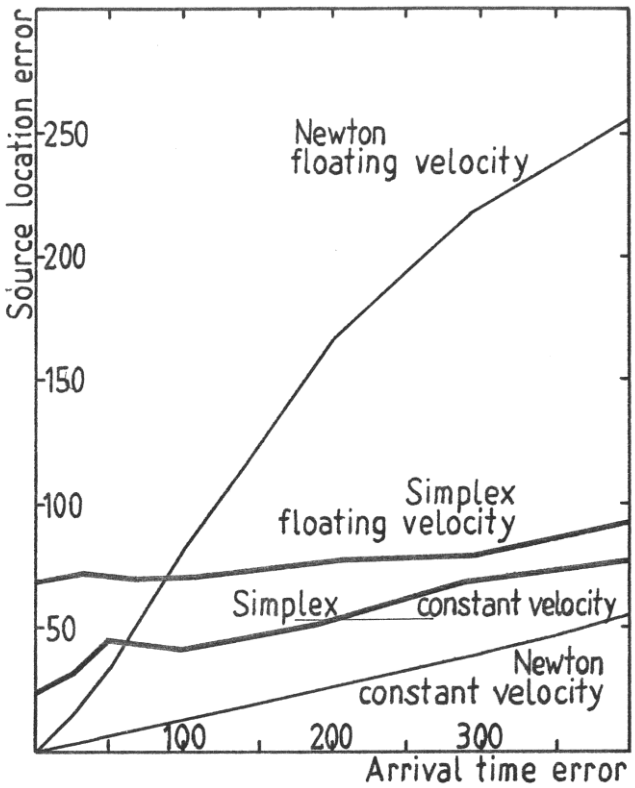


**Figure 8: Comparison of the error propagating properties of the Newton Least Squares and the Simplex methods for three-dimensional source location. (after Collins and Belchamber, reference 149).**

## 4.5 Applications of AESL

Typical applications of acoustic emission source location techniques for isotropic materials have included:

- Monitoring nuclear reactors during simulated operation [151-158]
- Hydroformer reactor shutdown and regeneration cycles [153]
- Hydrostatic testing of pressure vessels [125, 153-162]
- Hydrostatic testing of pressure pipeline segments [163]
- Highway industrial-gas trailer tubing [153]
- Railroad tank cars [164]
- Pipeline leak and defect detection [153, 165]
- Drilling rig blowout preventers [153, 166]
- Post-weld monitoring [167-168]
- Stress corrosion cracking in hot blast stove roofs [52]
- Stress corrosion microdamage due to hydrogen sulphide [169]
- Scaling corrosion of aluminium alloys [170]
- Full scale fatigue testing of airframe structures [171]

## 5 SOURCE LOCATION IN COMPOSITE MATERIALS

Fibre reinforced materials present additional complexities to the use of acoustic emission as a source location technique. The elastic properties of these materials change with the relative orientation of the wave propagation direction to the reinforcement direction. The attenuation of the signal is usually far greater than in metals. Harris and Phillips [172] have reported typical values for the wavespeed and attenuation of glass fibre reinforced plastics, as shown in Figure 9.

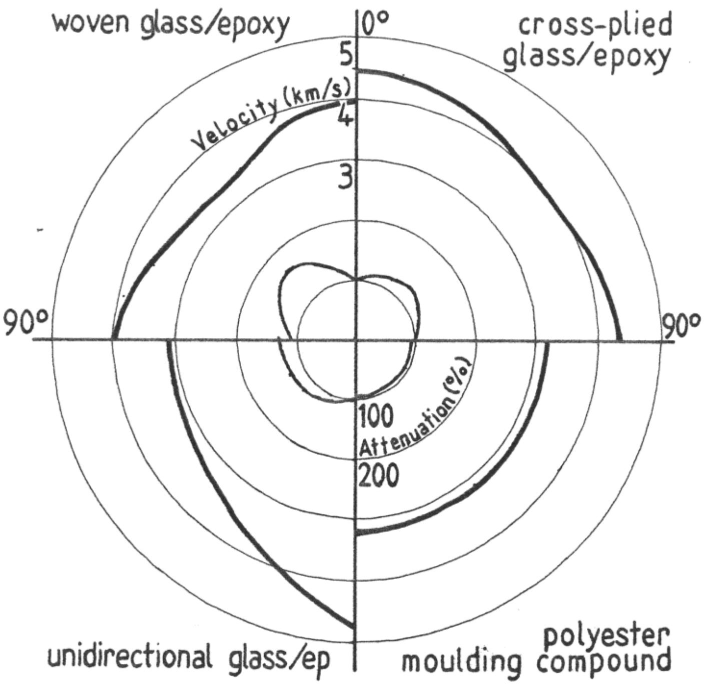


**Figure 9: Ultrasonic velocity (outer bold line) and attenuation (inner thin line) as a function of orientation in the plate for four different glass-fibre reinforced materials. (after Harris and Phillips, reference 172).**

The implications of this were highlighted by Hamstad [173] in 1983: "The classical techniques of source location ..... which result in a much more precise location have not yet been fully implemented in most composites".

Hamstad [174] studied the transient recorder waveforms for pencil lead break simulated AE signals on an aramid/epoxy composite. A significant amplitude difference was observed between the first half-cycle of the AE event and the peak amplitude of the event. Commercial AE instrumentation uses threshold crossing to determine the arrival time of an AE event. Accurate source location is thus particularly dependent on the peak amplitude for each channel of the array and on having a significantly large difference between the threshold and the peak amplitude. The study considered four factors:

- the AE signal background electronic noise,
- the rise of the AE event out of the background noise,
- the frequency band-pass of the AE system, and
- the relative positions of the source and sensors.

The key conclusions were:

- the difference (ΔdB) between the system threshold and the peak AE event amplitude must be large to ensure detection of the first real half-cycle of the signal.
- source location tests on composites should be run at maximum sensitivity to maximise the AE events obtained.
- increased sensitivity of AE systems may require new approaches to the determination of AE arrival times. These may include signal envelope techniques or 'smart' systems that would recognise and reject individual half-cycles of noise with high amplitudes.

### 5.1 Linear source location

Awerbuch *et al* [175] monitored monotonically increasing load and load/unload cycles to failure in cross-plied graphite/epoxy. AESL distribution histograms, correlated with X-radiographs, indicated that first ply failure (FPF) could be located in laminates with 90° surface layers, where failure is initiated by edge delamination propagating to the surface layers. With axial (0°) surface layers, emission occurred throughout the specimen length and FPF location by AESL was not possible.

Awerbuch *et al* [176] undertook a study of the viability of the Kaiser and Felicity Effects as a measure of damage severity. The material tested, unnotched or notched filament wound graphite epoxy, was loaded and unloaded between 8 to 12 times with incremental increases up to failure load. AESL distribution histograms revealed that emissions occurred throughout the specimen length as a result of fabrication inhomogeneity. In 'longitudinal' specimens with notches smaller than 10% of the specimen width, notches could not be detected or located. In 'transverse' (notch-sensitive) materials, notches could be easily detected and located. Similar experiments were conducted in fatigue loading [177], although as the number of cycles increased the contribution of friction between the fractured surfaces to the emission became dominant.

Madhukar and Awerbuch [178] plotted the AESL distribution histograms for centre-notched quasi-isotropic boron aluminium laminates in quasi-static tensile loading. Less than 20% of the events occurred in the notch region. Emissions were due primarily to matrix plastic deformation and interfacial failure. The smallest artificial notches which could be discriminated were again 10% of the total specimen width.

Awerbuch and coworkers [179-183] studied graphite/epoxy laminates in static loading and low-cycle fatigue. The samples were either double edge notched CFRP or non-visual impact-damaged laminates. Initial emissions were generated around the centre of the specimen (original damage or notch positions). Later in the fatigue tests, after extension of the splits, emissions were repeatedly recorded at specific locations along the splits, and these were attributed to fretting of the crack surfaces during crack closure. Most of the friction-generated events have intensities (count, duration or counts/event) below a FRiction Emission Threshold (FrET) value. By excluding events of intensity lower than the FrET value, it was possible to construct Derived-Damage (DD-) curves from the events generated primarily by the damage. The DD-curves permit more accurate determination of the damage accumulation.

Ghaffari and Awerbuch [184] have studied the initiation, accumulation and progression of matrix splitting in double edge notched unidirectional graphite/epoxy composites. During tensile testing, the growth of matrix splitting accounted for the acoustic emissions generated. However, "locating damage initiation and tracking its progression is not possible". If all four splits (one in each direction parallel to the fibres at each of the notches) progressed simultaneously, then only the longer split on each side could be tracked.

Wolters [185] tested model specimens consisting of single longitudinally aligned glass fibres (with diameters between 6-24 microns, and failure strains of 3-5%) in either a ductile polycarbonate (PC, yields at 6% strain, fails at 100% strain) or a brittle styrene-acrylonitrile (SAN, fails at 2.6% strain) polymer matrix. In PC, the fibre is progressively broken into shorter lengths until the pieces are too short to transmit the ultimate stress to the fibre. The AE locations were found all along the monitored length of the specimen. In SAN, the matrix crazes and the fibre fails when it is subjected to locally concentrated cracks. The regions of increased AE activity were correlated to the accumulation of crazes.

Shiwa *et al* [186] monitored acoustic emission during load-hold and unload-reload tests of 62 v/o plain-weave E-glass in epoxy resin. 'Cascade' plots of events against linear location (against stress-step) were widely distributed. Cascade plots of event energy (not defined) against the same parameters showed a few highly concentrated positions close to the highly-stressed parts of the sample, corresponding to the site of final failure.

Cherfaoui *et al* [187] monitored defect location in a three-point bend test on a unidirectional SMC-glass/epoxy beam with an embedded PTFE delamination. Initial AE locations were correlated with the end of the delamination or with known defects and confirmed visually. Defect behaviour could be analysed in real time.

Yamaguchi *et al* [188] conducted digital waveform analysis during tensile testing of waisted notched unidirectional 58 v/o glassfibre/epoxy composites. The plots of linear location against event number were grouped into four blocks of data points. The first two groups were associated with through-thickness splitting from the root of the notch, one split running in each direction on opposing edges of the sample. The later two groups were associated with delamination in the width of the sample.

Dorosh and Poursatip [189] monitored three-point bend fatigue tests on unidirectional GFRP pultruded rods and on cross-ply laminates with acoustic emission. The damage grew in length and depth from the tensile surface below the central load point. After suitable filtering, the AE monitoring could locate events generated along the damaged length during cycling. The extent of the event-location histogram was a direct measure of the damage length. Damage depth was indicated by the attenuation of the acoustic signal.

Hill *et al* [190] used linear location to show that throughout stress corrosion tests (random E-glass fibre/polyester resin in sulphuric acid) the acoustic emission was principally located at the notch. Samples pulled to failure after varying amounts of AE activity showed lower residual strengths with greater number of AE events recorded in the preceding stress corrosion test.

Inoue *et al* [191] tested specimens of fresh mature bovine tibia cortical bone (200 μm OD osteon: thick walled tubes filled with interstitial lamellae, connected internally and externally by a mucopolysaccharid cement: at the ultramicrostructural level both the osteon and lamella are collagen fibre reinforced hydroxyapatite matrix) in tension. The AE flaw locations for 0° and 90° specimens are plotted against strain and the line of final fracture in Figure 10.

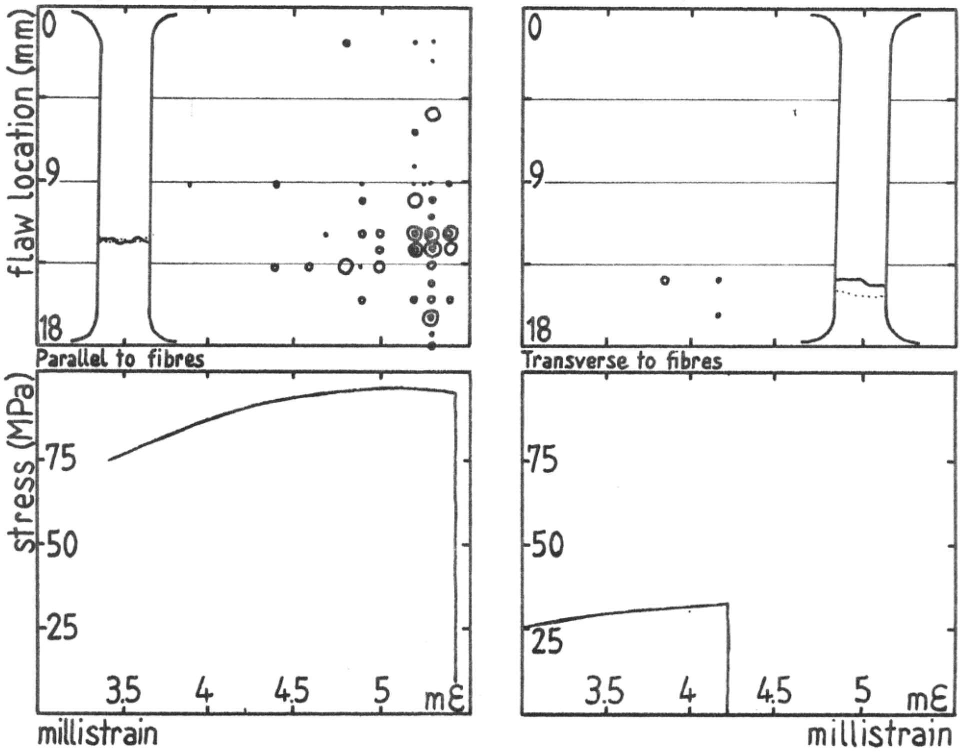


**Figure 10: Relation between stress-strain curves and AE source location for tensile tests parallel and transverse to the fibres. (after Inoue *et al*, reference 191).**

Rouby [192] used two 400 kHz resonant transducers for linear AESL to monitor fibre fractures in unidirectional Grafil-HT carbon-fibre reinforced DGEBA epoxy resin. Pencil breaking was used to calibrate the wave velocity (2075 ± 50 m/s) corresponding to the pressure wave. A typical example of the locations of successive events is given in Figure 11, with the location accuracy being of the order of 0.5 mm. Fracture can be seen to occur randomly along the fibres, with a succession of neighbouring events seldom observed.

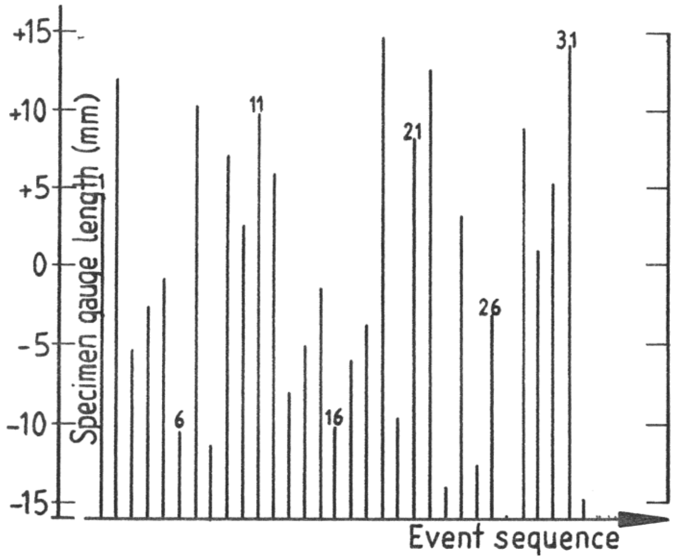


**Figure 11: Source location as a function of event number for a single-filament carbon-epoxy composite (after Rouby, reference 192).**

Weng *et al* [193] studied damage processes during cyclic deformation of notched short glass-fibre reinforced liquid crystal polyester (LCP) composites by linear AESL techniques. Visual and infra-red thermal imaging suggested that no stable crack propagation occurred. 'Cascade' linear location plots showed that damage in the composite was localised near the notch and somewhat broader in the neat LCP resin. The AE measurements suggested that failure occurred by a damage related micro-cracking mechanism during the final 20% of the cycling time.

Nishikawa *et al* [194] monitored and located fibre breaks in a single-fibre composite four-point bend test. Good agreement was obtained between the mean fragment length (625 μm) measured by an AESL technique and by an optical microscope technique. The AESL technique has the advantages that the cumulative AE event count indicates that fibre breaks have saturated, that opaque coupons can be monitored and the measurement can be faster and can be automated.

### 5.2 Areal source location

Early tests on planar source location for sandwich panels were performed by Kelly *et al* [195]. A 13 mm diameter flat-faced punch was forced into the cross-plied graphite/epoxy face sheets of a 13 mm thick honeycomb sandwich panel. Local failure occurred by fibre fracture, delamination in the face-sheet and debonding of the face from the core. The scatter in the detected locations was attributed to the inherent load spreading during failure of such sandwich panels.

Bailey, Hamilton and Pless [196] used a face-centred equilateral triangular array of four transducers for AE source location to monitor tensile tests of impact damaged and fatigued cross-plied carbon fibre/epoxy composites. The instrumentation was a Dunegan Endevco model 1032 with 100-700 kHz transducers. The source location algorithm was not indicated. By far the majority of the located flaws were situated around half-way between the apex of the triangle and the central transducer concentrated in a central vertical band corresponding to 35% of the width of the base of the array and in the position used for calibration or impact (Figure 12). Only a few scattered events originated in the larger area and numbers prior to specimen fracture were not significant.

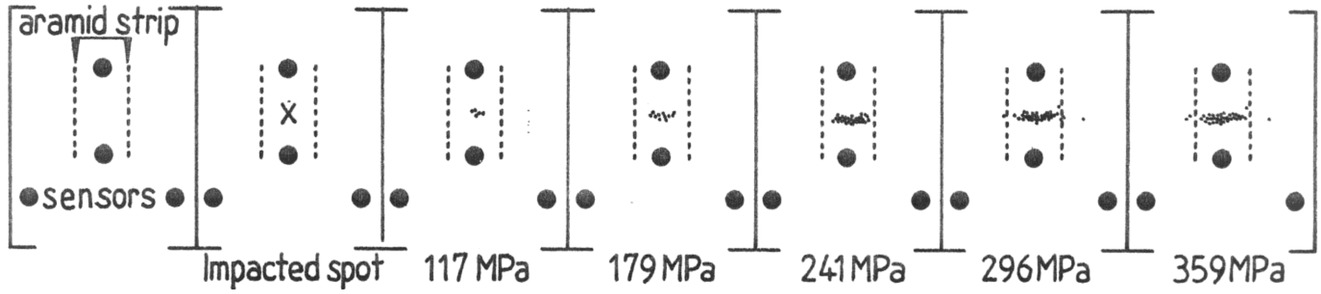


**Figure 12: Sequence of source locations displayed with increasing load. (after Bailey *et al*, reference 196).**

Bailey, Freeman and Hamilton [197] used 500-800 kHz transducers with the same triangular array and instrumentation set-up to successfully identify two forms of damage (resin cracking and fibre fracture) by comparison of the signal levels with an AE simulator. The simulated signal amplitude was greater than that for resin matrix cracking and lower than that for fibre fracture. In compression testing of a hat-section stiffened cross-plied CFRP panel, resin cracking towards the right-hand edge of the array occurred at around 50% of the ultimate load and was implicated in the panel failure. A picture-frame shear fatigue test of a cross-plied CFRP panel with an edge-notched central hole was monitored with two four-transducer triangular arrays. Resin cracking at the notch and parallel to the fibres occurred when the test machine was in compression (resulting in tension at the notch tip).

Glennie and Summerscales [198] studied the source location problem on 940 mm square plates of unidirectional glass fibre reinforced polyester. The instrumentation consisted of four 28 kHz resonant accelerometers (B&K type 4335) fed to individual conditioning amplifiers (B&K type 2626). The four signals were logged by individual transient recorders (Datalab DL905 single-channel and DL922 double-channel instruments). A Schmit trigger based on the SN7413N integrated circuit was used to prime the individual recorders simultaneously. Minimum resolution times were 0.2 μs and 0.05 μs respectively. Subsequently a four-channel waveform recorder (Datalab DL1200, minimum resolution 2.0 μs) became available allowing the Schmit trigger to be removed from the system. The resolution was reduced using the DL1200, but data acquisition was greatly simplified through the use of the 'roll-time' facility. At the end of the project, data was obtained automatically using direct interrogation by an HP85 desktop computer through the IEEE-488 bus.

The velocity profile was obtained experimentally from the first-peak of the wavefront. Hamstad [174] noted that such use of first half-cycle peak, rather than threshold penetration, may overcome rise-time effects. However no systematic research is known on the effect of rise time at various sensor frequencies on the accuracy of AESL in composites.

This velocity profile [198] was found to be a deformed ellipse, with an anisotropy ratio of 1.56 (4145m/s parallel to the fibres, 2655 m/s normal to the fibres) and flattened at angles other than the major and minor axes. Use of a circular wavefront AESL solution produced a distortion of the determined source location. Use of co-ordinate scaling to transpose the ellipse to a circle improved the accuracy considerably, but errors were still present due to the flattening of the ellipse. It was possible to locate the source within the accuracy of the equipment used by the use of scaled co-ordinates and a simple linear interpolation from a coarse rectangular grid of local errors.

Summerscales [199] has suggested a new model for the wavefront profile which may allow a more effective solution of the above AESL problem. The new equation is:

$$V = ellipse + variation \qquad \text{(Eq. 7)}$$
$$variation = A \cos(2n\alpha)$$

where 'ellipse' is the equation for an ellipse based on the measured velocities but reduced by half the amplitude of the variation at maximum velocity direction and increased by half the amplitude of the variation at minimum velocity direction, $A$ is the half-amplitude of the variation, $n$ is the directionality of the laminate (1 for unidirectional, 2 for bi-directional) and $\alpha$ is the angle subtended between the source transducer and the reference axis.

Ibitolu and Summerscales [200, 201] used the advanced instrumentation above to study the source location problem in woven roving fibreglass panels. The velocity profile in the material varied between 2800 m/s in the bias (45°) direction and 3330 m/s in the fibre directions. The anisotropy ratio was 1.19. With a square transducer array (parallel to the fibres) the velocity profile could be accurately modelled by an equation which is a specific form of equation 7:

$$V = R + A \cos 4\alpha \qquad \text{(Eq. 8)}$$

where $V$ is the velocity at an arbitrary angle, $R$ is the mean of the maximum and minimum velocities in the plane, $A$ is the half-amplitude of the variation and $\alpha$ is the angle subtended between the source transducer and the reference axis.

The source location was first calculated using the original Tobias algorithm. Velocities appropriate to the orientation of the source-transducer line to the reference axis were then calculated from the cosine function. The original Tobias algorithm was then used with the specific velocity-time parameters for each source-transducer delay.

Further tests were carried out with a diamond array (transducer array at 45° to the fibre axes). The wavefront profile model used was:

$$V = R - A \cos 4\alpha = R + A \cos 4(\alpha + 45°) \qquad \text{(Eq. 9)}$$

The new algorithm improved the accuracy of the source location. In all cases a single iteration was used, but it would be simple to modify the programme to perform multiple iterations until the convergence of the solution achieved the required accuracy. Careful attention must be paid to the definition of the material and array axes.

Buttle and Scruby [202] developed a two-dimensional location algorithm for composites with anisotropy ratio (AR) up to 3.8. Materials considered were biaxial glass (AR = 1.18), uniaxial glass (AR =1.60) and uniaxial CFRP (AR = 3.81). The algorithm incorporates the velocity dependence and requires the acoustic emission arrival times to calculate the source location using an iterative process. The location algorithm used the NAG Fortran Library Routine E04GEF [203, 204], a modified Gauss-Newton algorithm for finding the unconstrained minimum of a sum of squares of M nonlinear functions in N variables (M≥N) requiring first derivatives.

Artificial AE events were generated using a pulsed laser source. Location accuracies of ±0.4 mm, ±0.7 mm and ±3.0 mm were obtained for the three materials listed respectively (Table 1). Square and diamond arrangements of transducers were found to give a similar location accuracy. However the angular function chosen for the velocity was found to be important for rapid convergence of the location algorithm to the correct location.

***Table 1: Summary of areal source location in composites (with additional information from [205])***

| | ***Biaxial*** | ***GRP*** | ***Uniaxial*** | ***GRP*** | ***Uni.CFRP*** |
|---|---|---|---|---|---|
| Authors | Ibitolu | Buttle | Glennie | Buttle | Buttle |
| Date | 1987 | 1988 | 1985 | 1988 | 1988 |
| | | | | | |
| High speed (m/s) | 3330 | 4300 | 4145 | 4800 | 9350 |
| Low speed (m/s) | 2800 | 3650 | 2655 | 3000 | 2450 |
| Anisotropy ratio | 1.19 | 1.18 | 1.56 | 1.60 | 3.81 |
| | | | | | |
| Calibration AE.source | Pencil | Laser | Pencil | Laser | Laser |
| Array size (mm$^2$) | 180000 | 2480 | 247500 | 2550 | 5540 |
| Transducer frequency | 28 kHz | 7 MHz | 28 kHz | 7 MHz | 7 MHz |
| Transducer rise time | -- | 60 ns | -- | 60 ns | 60 ns |
| Transducer diameter | 14 mm | 1 mm | 14 mm | 1 mm | 1 mm |
| | | | | | |
| Sampling frequency | 500 kHz | 20 MHz | 500 kHz | 20 MHz | 20 MHz |
| Sampling resolution (μs) | 2 | 0.05 | 2 | 0.05 | 0.05 |
| | | | | | |
| Location accuracy (mm) | 10 | 0.4 | 10 | 0.7 | 3.0 |
| Plate thickness (mm) | 12 | 1.5 | 12 | 1.5 | 4.6 |

Castagnede *et al* [206] have presented an optimisation process for AE point source location in a homogeneous anisotropic material. For a 2-D plate with parallel surfaces, the solution yields a non-linear system of transcendental quadratic equations where the coefficients are functions of the unknowns themselves. To solve this over-determined system of non-linear equations a Euclidean functional $F(X_s, Y_s)$ was defined and then minimised using a modified Newton-Raphson numerical method. The robustness of the algorithm was demonstrated on results obtained in simulation with some characteristic features. The convergence performance decreased as the source was moved further from the centre of the sensor array. The coefficient of variation of the optimised co-ordinates was smaller than the perturbation on the time-of-flight differences whilst inside the sensor array.

This optimisation method has been applied to AESL in a 12 mm thick unidirectional glass fibre/(Extren 500 isophthalic) polyester resin composite with 80 μm OD capillary glass tube AE simulation [207]. The measurements were done in the near-field to limit the influence of attenuation and dispersion on the transient waves. When moving to the far-field, plate modes with stronger amplitudes can become problematic.

Bouheraoua [208, 209] has described a system for AESL on strongly anisotropic composite materials, based on a learning principle. The structure was calibrated by use of an electric arc at each nodal point, with digitised co-ordinates, amplitudes and delta-time values transferred to the computer. An attenuation grid was included for amplitude correction of each event. The accuracy was better than 10 mm, using a 20 mm step length and 1 μs resolution.

### 5.3 Location on spherical composite surfaces

Whittaker *et al* [210] have reported results from a project to develop high-accuracy source location techniques for a small spherical vessel made by over-winding a pair of 2mm thick 57 mm diameter aluminium hemispheres with 4 mm thick Kevlar/epoxy. Pencil lead breaks showed that the AE signal propagated as symmetric and asymmetric Lamb waves with different velocities. These differences caused a linear increase in event rise time as propagation continued. The system described in section 4.3.1 [116, 117] was used to follow damage progression during pressure testing.

### 5.4 Volume location in composites

The Castagnede approach can be extended to the full 3-D problem by the inclusion of new fourth-degree terms in the set of non-linear equations [211]. A supplementary difficulty is the consideration of propagation in non-principal planes where analytical expressions for the slowness curves are not available. The eigenvalues of the Green-Christoffel propagation tensor should be numerically computed using a cyclic Jacobi method [212, 213]. In the general full 3-D case, a realistic approach implies several restrictions:

- measurements are made in a homogeneous elastic solid
- the directions of the principal acoustic axes must be known
- there must be knowledge of the elastic constants, or access to the acoustic parameters by calibration
- wave speeds of the quasi-modes for propagation in non-principal planes requires determination of the eigenvalues of the Green-Christoffel tensors
- the relative arrival times of particular wave modes must be accurately determined

In spite of these perceived restrictions and limitations, the method described was anticipated to be useful for monitoring the progression of failure in a composite structure.

### 5.5 Standardised procedures

The Committee on Acoustic Emission from Reinforced Plastics (CARP: a working group of the Corrosion-Resistant Structures Committee of the Reinforced Plastics/Composites Institute) at the Society of the Plastics Industry (SPI) first published procedures for the examination of fibre reinforced plastics vessels in 1982 [214]. The committee has since been transferred from SPI to the American Society for Nondestructive Testing (ASNT).

The procedures have been accepted, with minor variations, by both the American Society for Testing and Materials (ASTM) [215] and the American Society of Mechanical Engineers (ASME) [216, 217]. The codes are voluntary under SPI/ASNT and ASTM, but have the standing of state legislation under ASME.

One company was experiencing an average of two catastrophic vessel failures each year before implementation of acoustic emission testing in 1980. Only two tanks have subsequently failed in service over a seven year period [61]. AE testing had shown the two tanks to be unsafe for continued operation, and they were operating at reduced levels with appropriate precautions. The first predicted failure occurred before installation of the replacement vessel.

Standardised procedures have also been agreed for reinforced plastics piping [218, 219], oil exploration/exploitation downhole tubing [220-222] and aerial lift devices [223]. Conlisk [224] has suggested that the CARP codes for fully vented tanks may be applied to chemical resistant floor grating panels.

Slykhous [225] explored location techniques for straight lengths of RTR (reinforced thermosetting resin) pipe, in addition to the normal CARP criteria. First arrival location showed both speed and repeatability advantages over time-of-flight location. At less than 150 mm, exact source location was practical as attenuation and wave mode separation are not limiting at this distance. For very long sections of pipe, the water-borne signal could be used.

Exact location was used on an in-line pipe joint with good results due to the short distances involved. Two major velocities were identified, and both were used for the location solution. Data from the coupling itself, the O-ring area and the pipe-thread could be separated.

Fowler [226] conducted tests under the auspices of the ASTM committee on RTR downhole tubing and the CARP committee on calibration to cross-calibrate AE instrumentation supplied by different manufacturers. The CARP calibration procedures were shown to be important prerequisites to satisfactory AE testing, ensuring consistent results between different test instruments.

### 5.6 Applications of AESL on composite structures

Dean and Kerridge [43] developed an immersion technique for recording of the number, amplitude, spectral content and source location of acoustic emissions from carbon fibre reinforced epoxy model rocket motor cases of oblate spheroidal shape. Immersion transducers have a more linear amplitude and frequency response than surface mounted transducers, are more sensitive and are less likely to record multiple pulses from a single event. Analysis is simplified as only compression waves are transmitted in water. CFRP exhibits severe mechanical anisotropy (and hence acoustic velocity variation), high overall attenuation and selective frequency attenuation. Also, the difficulty of reliable and repeatable transducer coupling and multiple path transmission can cause confusion. The immersion transducer was located at the centre of the vessel and three conventional 2.5 MHz transducers were located on the external surface at 120° intervals around the equatorial plane. No source location results were reported.

McNally and Mitchell [227, 228] have demonstrated that acoustic emission monitoring may be used for locating defects and damage in graphite/epoxy composite rocket motor cases during pressurisation with water (hydrotest). Reasonable sensitivity was achieved with 150 kHz resonant sensors in a zone location configuration.

Whalley and Cole [229] monitored the static testing of a CFRP military aircraft wing (comprising spars, ribs and skins bolted together) with the Dunegan/Endevco 1032 computerised AE system. An attenuation and velocity survey was carried out radially at 100 mm and 300 mm distances from a central point at 15° intervals around the circle. Maximum propagation distance for calibration sources was 650 mm. The D/E 8000 system was used for location accuracy checks. In most areas of the array, location accuracy was within 50 mm. In one area, the $\Delta t$ at one sensor doubled, presumably due to detection of a different wave mode, shifting the detected location by 120 mm.

The Dunegan Dart-32 acoustic emission field test service [230] has been used to ensure that the wings of the prototype EAP experimental agile fighter aircraft did not incur damage during ground testing of a complete CFRP wing in a single 27-sensor test with simultaneous 'on-line' analysis. The residual stress was stated to be predicted to an accuracy of better than 10% at only 50% of the failure load.

Rodgers [231-233] has reported the use of an eight-channel AET 5000A system during limit load testing of an experimental composite aircraft wing structural segment. The component was fabricated with 0°/±45° AS-3501 carbon fibre/epoxy prepreg with integral stiffening features. Seven 175 kHz resonant transducers were used with pencil lead break calibration to define zones based on order sequence at the sensors. Source location events were defined by more than one sensor hit within 250 μs and were recorded with sequence of transducers excited, and relative arrival times. The program also recorded localised signals which had insufficient strength to propagate to other transducers, the number of first hit events and the total number of hits for each channel at the end of the 50% load hold and at failure. Most zone located events were detected near the inboard flange during compression loading in the area of ultimate failure with amplitudes indicative of fibre fracture.

Holroyd and Cox [234] considered AE monitoring for the detection and location of damage during rig-shop testing of large CFRP aero-engine components. The success of a time difference based location system using a distributed array and standard software required:

- discrete burst AE activity with sufficient time-separation of signals to isolate individual events
- accurate determination of burst time-of-arrival, and
- an identifiable velocity for the signal with either a circular or elliptical velocity profile

These assumptions were suspected to be invalid because:

- at high activity rates, the burst definition is unclear
- avalanches of closely spaced bursts may yield spurious locations
- several spatially separate sites may be active simultaneously
- the velocity profile is neither circular nor elliptical
- the signal is subject to high attenuation, and
- the sharp leading edge is subject to strong dispersion in plate-like composite structures

An 'attenuative isolation' technique using multiple high-frequency transducers was developed with good immunity from background noise and a capability to handle high rates of activity. The system employs preamplifier substations and disposable transducers. Material attenuation was characterised by computer-controlled mapping of a scanned gas jet.

## 6 SUMMARY

This monograph has considered calibration sources for acoustic emission (AE), source location (SL) philosophies and the application of AESL to defect and/or damage location in both isotropic and anisotropic materials and structures.

## 7 ACKNOWLEDGEMENTS

The author gratefully acknowledges Mr T F Drouillard (EG&G Rocky Flats Inc) and Mr Peter Senior (Loughborough University of Technology) for their invaluable help in locating the correct reference to Hoff [88], and Dr Chris Scruby for additional information to complete Table 1. Also to Joe Coutts for the translation of sections of Fontana [96].

## 8 REFERENCES

1 M Arrington "Acoustic emission"
Chapter 2 in J Summerscales (editor): 'NDT of FRP Composites 1'
Elsevier Applied Science Publishers, London, September 1987, 25-63.

2 TF Drouillard (edited FJ Laner) 'Acoustic emission - a bibliography with abstracts'
IFI/Plenum Data Co, New York, 1979.

3 TF Drouillard "AE literature"
Journal of Acoustic Emission, most issues.

4 [deleted].

5 HJ Rindorf 'Acoustic emission source location in theory and practice'
Bruel & Kjaer Technical Review, 1981, (2).

6 N Chretien and C Perennes "La localisation des sources d'emission acoutique"
Proc.Journees d'Etudes sur l'Emission Acoustique, INSA, Lyon, March 1975, pp 279-322.
Bulletin d'Informations Scientifiques et Techniques, CEA, February 1976, (211), 85-95.

7 A Nielsen "Acoustic emission detection during straining of steel"
RISO Report RISO-M-1290, September 1970.

8 A Nielsen "Acoustic emission source based on pencil lead breaking"
Svejsecentralen Kobenhavn (Danish Welding Institute) Report 80-15, 1980.

9 Code sub-group of the European Working Group on Acoustic Emission "Acoustic emission reference source"
NDT International, August 1981, 14(4), 184.

10 NN Hsu "Acoustic emissions simulator"
US Patent 4 018 084, filed 13 May 1976, published 19 April 1977.

11 "Standard guide for determining the reproducibility of acoustic emission sensor response"
ASTM Standard E976-84, 27 January 1984.

12 "Standard practice for acoustic emission examination of fibreglass reinforced plastic resin (FRP) tanks/vessels"
ASTM Standard E1067-85, 31 May 1985. [1990 Annual Book of ASTM Standards, Volume 03.03, pp 474-486]

13 'Boiler and Pressure Vessel Code' ASME, July 1983.

14 Y Higo and H Inaba "Characteristics of pencil lead for AE system calibration"
In K Yamaguchi, I Kimpara and Y Higo (editors): 'Progress in Acoustic Emission IV'.
Proc.8th.Intl.Acoustic Emission Symposium (IAES 9), JSNDI, Kobe, November 1988, pp 164-169.

15 Y Higo and H Inaba "The general problems of AE sensors"
Journal of Acoustic Emission, January-June 1989, 8(1/2), s24-s27.
Proc.World Meeting on Acoustic Emission, AEWG, Charlotte NC, 20-23 March 1989.

16 SC Cowin "A note on broken pencil points"
Trans.ASME Series E: J.Applied Mechanics, June 1983, 50(2), 453-454.

17 D Eitzen, F Breckenridge, R Clough, N Hsu, T Proctor and J Simmons
"NBS developments in quantitative acoustic emission measurements"
8th.Ann.Rev.Progress in Quantitative Non-Destructive Evaluation, USAF/DARPA, Boulder Co, August 1981.
Proceedings edited DO Thompson and DE Chimenti, Plenum NY, 1982, v1, pp 433-442.

18 FR Breckenridge, CE Tschiegg and M Greenspan "Acoustic emission: some applications of Lambs problem"
Journal of the Acoustical Society of America, March 1975, 57(3), 626-631.

19 H Lamb "On the propagation of tremors over the surface of an elastic solid"
Phil.Trans.Roy.Soc, September 1904, A203, 1-42.

20 CL Pekeris "The seismic surface pulse"
Proc.Nat.Acad.Sci., 15 July 1955, 41(7), 469-480.

21 FR Breckenridge "Acoustic emission transducer calibration by means of the seismic surface pulse"
Journal of Acoustic Emission, 1982, 1(2), 87-94.

22 "Standard method for primary calibration of acoustic emission sensors"
ASTM designation E1106-86, approved 25 April 1986.
23 RH Chambers and SA Hoenig "New techniques in NDT by acoustical and exo-electron emission"
University of Arizona Engineering Experiment Station report, 31 August 1969. NTIS AD 720 357.
24 LJ Graham "Acoustic emission transducer characterisation"
North American Rockwell Corporation Science Center report SCTR-71-19
Thousand Oaks CA 91360, December 1971
25 A Kamio "On the relation of a recorded value of acoustic emission to the sizes of cracks"
Hi-Hakai Kensa (Jap.J.NDI), August 1971, 20(8), 368-369.
26 CA Tatro "Design criteria for acoustic emission experimentation"
ASTM Special Technical Publication, 1972, STP 505, 84-99.
Proc.Symp.Acoustic Emission, ASTM, Bal Harbour, December 1971.
27 NI Dreiman "Sound emission by metals and alloys"
Industrial Laboratory, January 1972, 38(1), 52-54.
28 A Kanno, M Sakaki and K Katsumata "Correlation between acoustic emission and crack size calibrated by standard AE source generated by dropped steel ball"
Hi-Hakai Kensa (Jap J NDI), July 1974, 23(7), 357-363.
29 GJ Farrow and MI Darby 'Study of simulated acoustic emission in unidirectional carbon fibre reinforced plastic'
Journal of Physics D: Applied Physics, 14 February 1992, 25(2), 234-241.
30 PH Hutton and HN Pedersen "Crack detection in pressure piping by acoustic emission"
Battelle Northwest report BNWL-1187, September 1969, pages 3.1-3.18.
31 SL McBride and TS Hutchison "Helium gas jet spectral calibration of acoustic emission transducer and systems"
Canadian J Physics, 1 September 1976, 54(17), 1824-1830.
32 GA Green "Simple method for the direct comparison of acoustic emission detection systems"
Nondestructive Testing International, April 1978, 11(2), 69-71.
33 WF Hartman "Experiments with a portable acoustic emission simulator and calibration device"
12th meeting, AEWG, New York, December 1973.
34 DO Harris "The effects of gain and frequency bandpass on acoustic emission observed from growing fatigue cracks"
Dunegan Endevco Technical Report DE74-4, January 1974.
35 RL Bell "Acoustic emission transducer calibration: transient pulse method"
Materials Evaluation, September 1972, 30(9), 37A, abstract only.
32nd.National Fall Conference, ASNT, Cleveland OH, October 1972.
Dunegan Endevco Technical Report DE73-3, February 1973.
36 CC Feng "Acoustic emission transducer calibration: spark impulse calibration method"
Endevco Engineering report 74-7-C, 1974.
37 C Feng and RM Whittier
"Acoustic emission transducer calibration using transient surface waves and signal analysis"
In HL Dunegan and WF Hartman: 'Advances in Acoustic Emission',
Proc.1st Conf Acoustic Emission, ASNT, Anaheim, September 1979. Dunhart, Knoxville TN, 1981, pp 350-366.
38 DB Egle and AE Brown "A note on pseudo-acoustic emission sources"
Journal of Testing and Evaluation, May 1976, 4(3), 196-199.
39 RF Berry "Low cost calibration of acoustic locators"
NASA Tech Briefs, Summer 1980, 5(2), 169-170.
40 HL Dunegan and CA Tatro "Acoustic emission effects during mechanical deformation"
In RF Bunshah 'Techniques of Metals Research, volume 5, part 2'
Interscience Publishers, New York, 1971, Chapter 12, pp 273-312.
41 BJ Shaw "On the use of piezoelectric films for ultrasensitive strain gauges, metal failure warning devices and for acoustic emission"
Ultrasonics Symposium, IEEE, Monterey, November 1973, 237-239.
42 WC Leschek "Acoustic emission transducer calibration"
Materials Evaluation, February 1975, 33(2), 41-48.
43 DS Dean and LA Kerridge "An immersion technique for the detection of acoustic emission in carbon fibre reinforced plastic pressure vessels"
NDT International, October 1976, 9(5), 233-238.
44 H Hatano and E Mori "Acoustic emission transducer and its absolute calibration"
J Acoustical Society of America, February 1976, 59(2), 344-349.
45 M Mirabile "Acoustic emission: past experience within ECSC contracts and future trends"
Commission of the European Communities Technical Steel Research report EUR 7887 en,
January 1983.
46 H Hatano, Y Mori, T Kishi and K Yamaguchi "On NDIS 2109: methods for absolute calibration of acoustic emission transducers by reciprocity techniques"
Proc.4th.World Meeting of the Acoustic Emission Working Group (AEWG-35), ASNT, Boston MA,
September 1991, 147-154.

47 J Holt and DJ Goddard "Assessment of an acoustic emission transducer for waveguide application" Central Electricity Research Laboratories note RD-L-N3-76, Leatherhead, March 1976.

48 CB Scruby, HNG Wadley, RJ Dewhurst, DA Hutchins and SB Palmer "A laser-generated standard acoustic emission source" Materials Evaluation, December 1981, 39(13), 1250-1254.

49 ORF Rose "Point source representation for laser generated ultrasound" J Acoustical Society of America, 1984, 75(3), 723-732.

50 CB Scruby, RJ Dewhurst, DA Hutchins and SB Palmer "Quantitative studies of thermally generated elastic waves in laser irradiated metals" Journal of Applied Physics, 1980, 51(12), 6210-6216.

51 U Schliechert *et al* "Theoretical and experimental investigation of broadband thermoelastically generated ultrasonic pulses" Proc.Conf.Photoacoustics, Heidelberg, 1987.

52 JW Wagner and RE Green "Optical generation and detection of ultrasound with acousto-ultrasonic applications" In GL Workman (editor): 'Nondestructive Evaluation for Aerospace Requirements' Gordon & Breach Science Publishers, New York, 1989, 113-123.

53 AE Brown and RG Liptai "Round-Robin testing of acoustic emission source" ASTM Special Technical Publication, 1972, STP 505, 318-331. Proc.Symp.Acoustic Emission, ASTM, Bal Harbour, December 1971.

54 MA Hamstad University of Denver, unpublished research

55 CR Heiple, SH Carpenter and SS Christiansen "A calibration source for acoustic emission analysis" ASTM Special Technical Publication, 1991, STP 1077, 77-85. Proc.World Meeting on Acoustic Emission, AEWG, Charlotte NC, 20-23 March 1989.

56 D Birchon, R Dukes and J Taylor "Some aspects of defect location and assessment in pressure vessels using acoustic emission techniques" Proc.2nd.Inf.Conf.Pressure Vessel Technology, San Antonio, 1-4 October 1973, pages 669-684.

57 D Birchon "The potential of acoustic emission in NDT" British J Non-Destructive Testing, May 1976, 18(3), 66-71.

58 Y Higo and H Inaba "The general problems of AE sensors" ASTM Special Technical Publication, 1991, STP 1077, 7-24. Proc.World Meeting on Acoustic Emission, AEWG, Charlotte NC, 20-23 March 1989.

59 TJ Fowler "Acoustic emission testing of process industry vessels and piping" Proc.5th.Int.Symp.Loss Prevention and Safety Promotion in Process Industries, Cannes, September 1986, paper 51, pp 1-15. BL 5294.741

60 TJ Fowler "Experience with acoustic emission monitoring of chemical process industry vessels" In K Yamaguchi, K Aoki and T Kishi (editors): 'Progress in Acoustic Emission III'. Proc.8th.Intl.Acoustic Emission Symposium (IAES 8), JSNDI, Tokyo, October 1986, pp 150-162.

61 TJ Fowler "Acoustic emission testing of vessels and piping" Chemical Engineering Progress, May 1987, 83(5), 25-32.

62 TJ Fowler "AE testing of chemical process industry vessels" In M Onoe, K Yamaguchi and H Takahashi (editors): 'Progress in Acoustic Emission II' Proc.7th.Intl.Acoustic Emission Symposium (IAES 7), JSNDI, Zao, 23-26 October 1984, 421-449.

63 R Halmshaw 'Non-destructive Testing' Edward Arnold, London, 1987, page 286.

64 RWB Stephens and AA Pollock "Waveforms and frequency spectra of acoustic emission" J Acoustical Society of America, September 1971, 50(3(2)), 904-910.

65 KA Fowler and EP Papadakis "Observation and analysis of simulated ultrasonic AE waves in plates and complex structures" ASTM Special Technical Publication, 1972, STP 505, pages 222-237. Proc.Symp.Acoustic Emission, ASTM, Bal Harbour, December 1971.

66 DK Hsu and H Jeong "Ultrasonic velocity change and dispersion due to porosity in composite laminates" Proc.15th.Annual Review of Progress in Quantitative Nondestructive Evaluation, 1988, 8B, 1567-1573.

67 JF Muratore and HR Carleton "Phase spectroscopy in lossy media" Ultrasonics Symposium, IEEE, 1985, 1047-1051.

68 Y Li and RB Thompson "Effects of pulse distortion on phase velocity measurements using the zero-crossing shift technique" Proc.16th.Annual Review of Progress in Quantitative Nondestructive Evaluation, Brunswick ME, 23-28 July 1989, volume 9, 203-210. Plenum Press, New York, 1990.

69 T-T Wu and Z-H Ho "Anisotropic wave propagation and its applications to NDE of composite materials" Experimental Mechanics, December 1990, 30(4), 313-318.

70 OI Sleptsov and AM Zhirkov
"Localisation of acoustic emission sources by the successive approximation method"
Tekhnicheskaya Diagnostika i Nerazrushayushchii Kontrol', 1990, 2(3), 75-79.
Technical Diagnostics & Nondestructive Testing, 1990, 2(3), 222-225.
71 I Grabec and W Sachse "Application of an intelligent signal processing system to acoustic emission analysis"
In K Yamaguchi, I Kimpara and Y Higo (editors): 'Progress in Acoustic Emission IV'.
Proc.8th.Intl.Acoustic Emission Symposium (IAES 9), JSNDI, Kobe, November 1988, pp 75-80.
72 C Eckart "The theory of noise in continuous media"
J Acoustical Society of America, 2 March 1953, 25(2), 195-199.
73 BF Cron and CH Sherman "Spatial correlation functions for various noise models"
J Acoustical Society of America, November 1962, 34(11), 1732-1736.
74 I Grabec "Application of correlation techniques for localisation of AE sources"
Ultrasonics, May 1978, 16(3), 111-115.
75 A-H Engelhardt "Beitrag zur Ortung von Schallemissionsquellen"
Dissertation, Abt. Maschinebau @ Univ. Dortmund, 1984.
76 M Klein "Ortung kontinuierlicher Schallemission mit 'phasengesteuerten' Gruppenemfangern"
Diplomarbeit, Fachrichtung 12.1: Werkstoffwissenschaften, Univ Saarbrucken, 1986.
77 P Holler and E Waschkies "Advanced methods and equipment for acoustic emission testing"
In J Eisenblatter (editor): 'Acoustic Emission',
DGM Informationsgesellschaft mbH, Oberursel, 1988, pages 3-23. ISBN 3-88355-131-7.
78 JF Nankivell "An evaluation of accuracies in source location using acoustic emission"
Proc.4th.Pan-Pacific Conference on Nondestructive Testing, 1983, Paper AE6, pages 1-8.
79 JF Nankivell "An evaluation of accuracies in source location using acoustic emission"
Non-Destructive Testing, September-October 1984, 21(5), 9-11.
80 European Working Group on Acoustic Emission
"The EWGAE Code for acoustic emission examination - location of sources of discrete acoustic events"
NDT International, August 1981, 14(4), 181-184 [13].
81 "Standard recommended practice for AE monitoring of structures during controlled stimulation"
ASTM E569-78, 1976.
82 TF Drouillard Private communication, 8 November 1991.
83 AM Vasil'ev and B Ya Maslov "Selection of the number of receiving channels for an acoustic emission locator"
Defektoskopiya, January 1980, (1), 40-47.
Soviet Journal of Nondestructive Testing, 1980, 16(1), 29-34.
84 B Ya Maslov and AM Vasil'ev
"Analysis of the errors of location of acoustic-emission sources for one-dimensional objects"
Defektoskopiya, January 1983, 19(1), 59-64.
Soviet Journal of Nondestructive Testing, January 1983, 19(1), 49-53
85 HH Moeller, T Powers, DR Petrak and JE Coulter
"Study of crack growth in structural ceramics using AE location techniques"
SAMPE Quarterly, July 1985, 16(4), 44-48.
86 I Grabec and W Sachse "Application of an intelligent signal processing system to acoustic emission analysis"
J Acoustical Society of America, March 1989, 85(3), 1226-1236.
Cornell University Materials Science Centre Report 6428, April 1988.
87 HR Hardy, F Taioli and ME Hager
"Use of mechanical waveguides and acoustic antennae in geotechnical AE/MS studies"
Journal of Acoustic Emission, January-June 1989, 8(1/2), s42-s48.
Proc.World Meeting on Acoustic Emission, AEWG, Charlotte NC, 20-23 March 1989.
88 M Hoff "Acoustic emission source location using single and multiple transducer arrays"
Proc.Ultrasonics Symposium, IEEE, Boston MA, October 1972. Catalogue no: 72 CHO 708-8 SU, pages 8-12.
[Note: this appears to be the correct reference for WC Patthoff,
Welding Journal, 1959, 38(supplement), as quoted in 89]
89 RWB Stephens and HC Kim "Acoustic emission: a diagnostic tool in non-destructive testing"
Chapter 12 in J Szilard (editor): 'Ultrasonic Testing: Non-Conventional Testing Techniques'
Wiley-Interscience, Chichester, 1982, page 491, reference 39.
90 A Tobias "Acoustic emission source location in two dimensions by an array of three or four transducers"
CEGB Berkeley Nuclear Laboratories report RD/B/N 3218, 1975.
91 A Tobias "Acoustic emission source location in two dimensions by an array of three transducers"
NDT International, February 1976, 9(1), 9-12.
92 A Tobias "ACEMAN - a PDP 11 operating system for acoustic emission analysis"
CEGB Berkeley Nuclear Laboratories report RD/B/N 3188, 1974.
93 ACE Sinclair "Acoustic emission techniques for in-service non-destructive examination: fatigue and creep"
CEGB Berkeley Nuclear Laboratories Report RD/B/N 4066, October 1977.
94 RL Bell
"A progress report on the use of acoustic emission to detect incipient failure in nuclear pressure vessels"

Nuclear Safety, September-October 1974, 15(5), 554-571.
95 N Chretien and C Perennes "La localisation des sources d'emission acoustiques"
Bulletin d'Information Scientifiques et Techniques, February 1976, (211), 85-95.
96 E Fontana, G Grugni, B Pirovano, G Possa and F Tonolini "Controllo non distruttivo di recipienti a pressione mediante analisi dell'emissione acustica nel corso della prova a pressione idrostatica"
Energia Nucleare, October 1974, 21(10), 550-558 (in Italian).
97 E Fontana, G Grugni, C Panzani, B Pirovano, G Possa and F Tonolini
"Acoustic emission monitoring during hydrotests of a thin wall pressure vessel"
Energia Nucleare, May 1975, 22(5), 253-259.
98 S Golinelli "A microcomputer in an acoustic emission source location system"
Energia Nucleare, December 1975, 22(12), 642-646.
99 M Onoe, K Yamaguchi, H Ichikawa and T Shimada "A multichannel acoustic emission source location system and its application to fatigue test of a reactor vessel"
Denki Gakkai Ronbunshi, June 1975, 95-C(6), 139-146.
Electrical Engineering in Japan, June 1975, 95-C(3), 129-137.
100 H Hatano, T Hanajima and N Niwa "Acoustic emission source location using 'face-centred' transducer arrays"
Transactions of Institute of Electronics and Communication Engineers of Japan:
Denshi Joho Tsushin Gakkaishi, October 1978, J61-C(10), 644-650.
Trans.IECE Japan Section E (English), October 1978, E61(10), 860-861
Electronics and Communications in Japan, October 1978, 61C(10), 97-104
101 VK Anisimov, VE Vainberg and VN Sosedov
"Method of determining the co-ordinates of sources of discrete acoustic emission signals"
Otkrytiya Izobreteniya Promyshlennye Obraztsy Tovarnye Znaki, 1980, (12), 188. Abstract only.
In Russian. (Inventors Certificate number 725 016). Translation T-7429, 1984.
102 VK Anisimov "Instantaneous determination of the locations of acoustic-emission sources in two co-ordinates"
Defektoskopiya, 1980, (8), 66-69.
103 AK Anisimov "Unambiguous determination of the co-ordinates of acoustic emission sources in sheet materials"
Defektoskopiya, July 1990, (7), 11-15.
Soviet Journal of Nondestructive Testing, 1991, 26(7), 446-450.
104 VE Vainberg and LI Dekhtyar'
"Computer-free method for determining the co-ordinates of an acoustic emission system"
Zavodskaya Laboratoriya, January 1982, 48(1), 40-43.
Industrial Laboratory, January 1982, 48(1), 41-45.
105 M Barsky and NN Hsu "A simple and effective acoustic emission source location system"
Materials Evaluation, January 1985, 43(1), 108-110.
106 OI Khol'kin "Location information of acoustic emission signals"
Defektoskopiya, February 1983, (2), 32-40.
Soviet Jnl of Nondestructive Testing, February 1983, 19(2), 105-111.
107 Y Obata, Y Mori and K Aoki "Evaluation of fatigue crack tip configuration in thick specimen by acoustic emission source location"
In K Yamaguchi, K Aoki and T Kishi (editors): 'Progress in Acoustic Emission III'.
Proc.8th.International Acoustic Emission Symposium (IAES 8), JSNDI, Tokyo, October 1986, pp 42-47.
108 MN Bassim and M Houssny-Emam "Time and frequency analysis of acoustic emission signals"
In JR Matthews (editor): 'Acoustic Emission', Gordon and Breach Science, New York, 1983, pages 139-163.
109 AN Podgornyi and IS Guz'
"Defect co-ordinates on the surface of spherical parts by the acoustic emission method"
Problemy Prochnosti, March 1977, (3), 33-37. Strength of Materials, March 1977, 9(3), 278-283.
110 M Asty "Acoustic emission source location on a spherical or plane surface"
NDT International, October 1978, 11(5), 223-226.
111 VK Anisimov "Application of the method of comparison to the localisation of sources of signals of acoustic emission on conical and spherical surfaces"
Defektoskopiya, 1981, (9), 96-98.
112 VK Anisimov "Investigation of the error of 'instantaneous' determination of the co-ordinates of sources of signals of acoustic emission on developable surfaces"
Defektoskopiya, 1981, (10), 106-109.
113 VK Anisimov "Investigation of the error of 'instantaneous' determination of the co-ordinates of sources of signals of acoustic emission on a segment of a spherical surface"
Defektoskopiya, 1981, (11), 108-111.
114 VK Anisimov "Approximate determination of the position of sources of acoustic emission"
Defektoskopiya, August 1988, (8), 49-52. Soviet J Nondestructive Testing, 1989, 24(8), 537-540.

115 H Nakasa "Acoustic emission source location for 3-dimensional structural components"
In K Yamaguchi, K Aoki and T Kishi (editors): 'Progress in Acoustic Emission III'.
Proc.8th.International Acoustic Emission Symposium (IAES 8), JSNDI, Tokyo, October 1986, pp 34-41.
116 O Burenko and JW Whittaker "Acoustic emission point source location on a thin spherical shell"
Proc.Southeastcon '87, IEEE, Tampa FL, 5-8 April 1987, volume 2, 546-552.
117 O Burenko and JW Whittaker "Graphics of acoustic emission point source location"
Proc.Conf.Energy and Information Technologies/Southeastcon '89, University of South Carolina,
9-12 April 1989, Session 11B7, pages 660-664.
118 D-J Yoon, YH Kim and O-Y Kwon "A simplified AE source location technique in the cylindrical vessel"
Proc.10th.International Acoustic Emission Symposium (IAES-10), JSNDI, Sendai, October 1990, 354-360.
119 D-J Yoon, YH Kim and O-Y Kwon
"New algorithm for acoustic emission source location in cylindrical structures"
Journal of Acoustic Emission, 1991, 9(4), 237-241.
120 DL Parry "Industrial applications of AE analysis technology"
ASTM Special Technical Publication, 1975, STP 571, 150-183.
Proc.Symp.Monitoring Structural Integrity by Acoustic Emission, ASTM, Fort Lauderdale, January 1974.
121 T Watanabe, S Hashirizaki and H Arita
"Acoustic emission inspection during water-pressure testing of pressure vessels"
NDT International, October 1976, 9(5), 227-232.
122 CR Horak and AF Weyhreter "Acoustic emission system for monitoring components and structures in a severe fatigue noise environment"
Materials Evaluation, May 1977, 35(5), 59-63+68.
123 H Kuehnicke, G Mauersberger and M Schade "Single-channel acoustic emission source locating technique"
Kernenergie, August 1979, 22(8), 271-273, Translation DRIC-T-7557.
124 H-A Crostack and A-H Engelhardt "Reducing the influence of wave modes and sound velocities on the location of acoustic emission sources"
In RB Clough (editor) (1983), pp 349-351, Proc.5th.Conf.NDE in the Nuclear Industry, San Diego, May 1982.
125 TJ Fowler, JA Blessing, PJ Conlisk and TL Swanson "The MONPAC system"
Journal of Acoustic Emission, July-September 1989, 8(3), 1-8.
Proc.World Meeting on Acoustic Emission, AEWG, Charlotte NC, 20-23 March 1989.
126 PT Cole "LOCAN acoustic emission system"
Private communication, 13 November 1986.
127 "LOCAN AT" Physical Acoustics Corporation, Princeton NJ 08543, 1988.
128 M Arrington Speedtronics Limited literature, undated.
129 "AET 5000B computer based acoustic emission system"
Acoustic Emission Technology Corporation, Sacramento CA 95815, 8 August 1986.
130 "Intuitive sensor system"
Stresswave Technology Limited ref 809.0004/B, Wirksworth UK, 1991.
131 TJ Holroyd, TE Tracey, N Randall and SD King "Stress wave sensing: affordable AE for industry"
ASTM Special Technical Publication, 1991, STP 1077, 25-34.
Proc.World Meeting on Acoustic Emission, AEWG, Charlotte NC, 20-23 March 1989.
132 TJ Holroyd and N Randall "Stress wave sensing - an approach to monitoring composite structures using simple integrated acoustic emission systems"
Stresswave Technology Limited paper, 1991.
133 VK Anisimov "A procedure for determining the co-ordinates of sources of acoustic-emission signals"
Byull.Izobret., 1980, (7), 251. (Inventors Certificate number 717648).
134 VK Anisimov "Instantaneous determination of the location of acoustic-emission sources in three co-ordinates"
Defektoskopiya, March 1982, (3), 8-11. Soviet J of Nondestructive Testing, 1982, 18(3), 162-165.
135 BYa Maslov and AM Vasil'ev "Determination of acoustic emission sources in three-dimensional space"
Defektoskopiya, March 1982, (3), 17-19. Soviet J of Nondestructive Testing, March 1982, 18(3), 172-174.
136 CB Scruby, KA Stacey and GR Baldwin "Defect characterisation in three dimensions by acoustic emission"
Journal of Physics D: Applied Physics, 19 September 1986, 19(9), 1597-1612.
137 KH Kim, T Nagumo, M Enoki, S Wakayama, T Kishi, T Oka and J Takatsubo
"Three-dimensional AE source location during fracture toughness testing in metals and ceramics"
In K Yamaguchi, K Aoki and T Kishi (editors): 'Progress in Acoustic Emission III'
Proc. 8th. Int.Acoustic Emission Symposium (IAES 8), JSNDI, Tokyo, October 1986, pages 48-57.
138 T Kishi and M Enoki "Three-dimensional location, dynamic Green's function and source moment tensor in acoustic emission signal analysis"
In J Eisenblatter (editor): 'Acoustic Emission',
DGM Informationsgesellschaft mbH, Oberursel, 1988, pages 25-36. ISBN 3-88355-131-7.
139 T Kishi and M Enoki "Three-dimensional location and source characterisation of microcracking in ceramics evaluated by AE signal analysis"
Proc. Conf. Nondestructive Testing of High Performance Ceramics,
American Ceramics Society, Boston MA, August 1987, pages 442-456.

140 K Nagano, H Niitsuma and N Chubachi
"A new automatic AE source location algorithm for downhole tri-axial AE measurement"
In K Yamaguchi, K Aoki and T Kishi (editors): 'Progress in Acoustic Emission III'
Proc. 8th. Int.Acoustic Emission Symposium (IAES 8), JSNDI, Tokyo, October 1986, pages 396-406.
141 K Nagano, H Niitsuma and N Chubachi
"Automatic algorithm for tri-axial hodogram source location in downhole AE measurement"
Geophysics, 1989, 54(4), 508-513.
142 K Nagano, H Niitsuma, M Sako and N Chubachi
"Confidence evaluating parameters for automatic source location in downhole AE measurements"
In K Yamaguchi, I Kimpara and Y Higo (editors): 'Progress in Acoustic Emission IV',
Proc.9th.International Acoustic Emission Symposium (IAES 9), JSNDI, Kobe, November 1988, 311-319.
143 IC Getting, C Roecken and H Spetzler "Improved acoustic emission locations"
Journal of Nondestructive Evaluation, 1986, 5(3/4), 133-143.
144 JF Labuz, HS Chang, CH Dowding and SP Shah
"Parametric study of acoustic emission location using only four sensors"
Rock Mechanics and Rock Engineering, 1988, 21(2), 139-148.
145 SC Maxwell, RP Young and DA Hutchins
"Simultaneous velocity tomography and source location of synthetic acoustic emission data"
ASTM Special Technical Publication, 1991, STP 1077, 86-94.
Proc.World Meeting on Acoustic Emission, AEWG, Charlotte NC, 20-23 March 1989.
146 Maochen Ge and HR Hardy "Design of 3-dimensional transducers arrays: theory and strategy"
Proc.World Meeting on Acoustic Emission, AEWG, Charlotte NC, 20-23 March 1989.
Journal of Acoustic Emission, January-June 1989, 8(1/2), s32-s37.
147 FR Redfern and RD Munson "Acoustic emission source location: a mathematical analysis"
US Bureau of Mines Report of Investigations 8692, 1982.
148 JA Nelder and R Mead "A simplex method for function minimization"
Computer Journal, January 1965, 7(4), 308-313.
149 MP Collins and RM Belchamber "Acoustic emission source location using simplex optimisation"
Journal of Acoustic Emission, 1991, 9(4), 271-276.
150 D Betteridge, AP Wade and AG Howard "Reflections on the modified simplex, I & II"
Talanta, 1985, 32(8B), 709-734.
151 WD Jolly "Field evaluation of a prototype acoustic emission reactor surveillance system"
Materials Evaluation, February 1973, 31(2), 29A.
152 MR Compton "A real time software operating system for a computer-controlled acoustic emission flaw monitor"
Materials Evaluation, February 1973, 31(2), 30A.
153 AT Green 'Nondestructive Testing Handbook, second edition'
American Society for Nondestructive Testing, Columbus OH, 1987,
Volume 5, Section 7, pages 155-223. ISBN 0-931403-02-2.
154 BH Schofield "A study of the applicability of AE to pressure vessel testing"
AFML-TR-66-92, April 1966. AD 809 369.
155 EV Waite and DL Parry "Field evaluation of heavy-walled pressure vessels using acoustic emission analysis"
Materials Evaluation, June 1971, 29(6), 117-124.
156 "Reactor pressure vessel integrity: in-service examination"
Nuclear Engineering International, September 1974, 19(220), 757-761.
[Report: IMechE Conf. Periodic inspection of pressurized components, London, June 1974]
157 T Watanabe, S Hashirizaki and H Arita "Flaw inspection test of large spherical tanks by AE technique"
Proc.2nd.AE Symposium, Tokyo, September 1974.
158 T Fuji and E Yamamoto
"Simplified multichannnel AE equipment for the testing of spherical high pressure tanks"
Proc.2nd.AE Symposium, Tokyo, September 1974.
159 E Fontana, G Grugni, B Pirovano, G Possa and F Tonolini "Controllo non distruttivo di recipienti a pressione mediante analisi dell'emissione acustica nel corso della prova a pressione idrostatica"
Energia Nucleare, October 1974, 21(10), 550-558. In Italian.
160 H Hatano "Acoustic emission: its fundamentals and applications"
Oyo Buturi, 1975, 44(6), 564-576.
161 R Davies "Acoustic emission as a basis for plant integrity monitoring"
In K Yamaguchi, K Aoki and T Kishi (editors): 'Progress in Acoustic Emission III'.
Proc.8th.International Acoustic Emission Symposium (IAES 8), JSNDI, Tokyo, October 1986, pp 9-25.
162 G Shen, S Liu, Y Wan and Q Duan "The correlation between active defects and source location in acoustic emission test of metal pressure vessels"
In K Yamaguchi, I Kimpara and Y Higo (editors): 'Progress in Acoustic Emission IV',
Proc.9th.International Acoustic Emission Symposium (IAES 9), JSNDI, Kobe, November 1988, 420-427.
163 PH Hutton and JB Vetrano "Crack detection in pressure piping by AE"
Battelle Northwest report BNWL-1315-2, 1970.

164 TJ Fowler "Recent developments in acoustic emission testing of chemical process equipment"
In K Yamaguchi, I Kimpara and Y Higo (editors): 'Progress in Acoustic Emission IV',
Proc.9th.International Acoustic Emission Symposium (IAES 9), JSNDI, Kobe, November 1988, 391-404.

165 DL Robinson and HR Devereaux "The application of acoustic techniques for the integrity analysis of piping"
Materials Evaluation, September 1973, 31(9), 38A.

166 "Acoustic emission of blowout preventers"
Acoustic Emission Working Group code case BCB2-727 section V, 1985.

167 WF Hartman "Acoustic emission detection of flaws in butt-welded plates"
Materials Evaluation, September 1973, 31(9), 38A-39A.

168 MN Bassim, DR Hay and M Talerman "Postweld evaluation by acoustic emission"
Materials Evaluation, May 1979, 37(6), 49-54.

169 H-A Crostack and P Bohm
"Investigations of hydrogen embrittlement at a sour gas vessel by means of a new location method"
In J Eisenblatter (editor): 'Acoustic Emission',
DGM Informationsgesellschaft mbH, Oberursel, 1988, pages 235-246. ISBN 3-88355-131-7.

170 AV Bakulin, SN Isaev and AP Tishkin "Acoustic emission location of corrosion centres"
Zashchita Metallov, November/December 1988, 24(6), 1017-1020. Protection of Metals, 1988, 24(6), 806-809.

171 D Bozzetti, A Sala, G Borzacchiello and C Sabatino
"AE monitoring of airframe structure during full scale fatigue test"
In K Yamaguchi, I Kimpara and Y Higo (editors): 'Progress in Acoustic Emission IV'.
Proc 9th.International Acoustic Emission Symposium (IAES 9), JSNDI, Kobe, November 1988, pages 454-461.

172 B Harris and MG Phillips "Non-destructive evaluation of the quality and integrity of reinforced plastics"
In B Harris (editor): 'Developments in GRP Technology 1', Elsevier Applied Science, London, 1983, pp 191-247.

173 MA Hamstad "Quality control and non-destructive evaluation techniques for composites, Part VI:
acoustic emission - a state-of-the-art review"
USAAVRADCOM Report TR-83-F-7, May 1983. AMMRC-TR-83-25. AD A132 621. N84-14245.

174 A Hamstad "On determination of arrival times for acoustic emission source location in composites"
Proc.2nd.Int.Symp.Acoustic Emission from Reinforced Composites, Montreal, July 1986, Session 7, 202-208.
Martin Marietta Oak Ridge Y-12 Plant report Y/SUB/86-19Y27448/1, 26 March 1986.
[CONF-860750-1. DE86 012964]

175 J Awerbuch, J Block and R Prinz
"Effect of stacking sequence in cross-ply graphite/epoxy laminates on acoustic emission results"
In T Hayashi, K Kawata and S Umekawa (editors):
'Progress in Science and Engineering of Composites', Proc.ICCM 4, Tokyo, October 1982, 1551-1555.

176 J Awerbuch, MR Gorman and M Madhukar "Monitoring acoustic emission during quasi-static loading/unloading cycles of filament-wound graphite-epoxy laminate coupons"
Proc.1st.Int.Symp.Acoustic Emission from Reinforced Composites,
SPI, San Francisco, July 1983, Session 3 @ 9:45, 1-19.

177 J Awerbuch, MR Gorman and M Madhukar "Monitoring damage accumulation in filament-wound graphite-epoxy laminate coupons during fatigue loading through acoustic emission"
Proc.1st.Int.Symp.Acoustic Emission from Reinforced Composites,
SPI, San Francisco, July 1983, Session 3 @ 3:25, 1-30.

178 M Madhukar and J Awerbuch "Monitoring damage progression in centre-notched boron/aluminium laminates through acoustic emission"
ASTM Special Technical Publication, 1986, STP 893, 337-367.
Proc.7th.Conference on Composite Materials: Testing and Design, Philadelphia, April 1984.

179 J Awerbuch and S Ghaffari "Monitoring progression of matrix splitting during fatigue loading through acoustic emission in notched unidirectional graphite/epoxy composites"
Proc.2nd.Int.Symp.Acoustic Emission from Reinforced Composites, SPI, Montreal, July 1986, Session 2, 51-58.

180 WE Eckles and J Awerbuch
"Monitoring acoustic emission in cross-ply graphite/epoxy laminates during fatigue loading"
Proc.2nd.Int.Symp.Acoustic Emission from Reinforced Composites, SPI, Montreal, July 1986, Session 3, 78-84.

181 S Ghaffari and J Awerbuch
"Monitoring acoustic emission in impact damaged composites"
Proc.2nd.Int.Symp.Acoustic Emission from Reinforced Composites,
SPI, Montreal, July 1986, Session 4, 120-125.

182 J Awerbuch and S Ghaffari "Tracking progression of matrix splitting during static loading through acoustic emission in notched unidirectional graphite/epoxy composites"
In K Yamaguchi, K Aoki and T Kishi (editors): 'Progress in Acoustic Emission III'.
Proc.8th.International Acoustic Emission Symposium (IAES 8),
JSNDI, Tokyo, 21-24 October 1986, pages 575-585.

183 J Awerbuch and S Ghaffari "Effect of friction-generated emission on monitoring damage in composite laminates through acoustic emission"
In K Yamaguchi, K Aoki and T Kishi (editors): 'Progress in Acoustic Emission III'.

Proc.8th.International Acoustic Emission Symposium (IAES 8),
JSNDI, Tokyo, 21-24 October 1986, pages 638-652.
184 S Ghaffari and J Awerbuch "On the correlation between acoustic emission and progression of matrix splitting in a unidirectional graphite/epoxy composite"
ASTM Special Technical Publication, 1991, STP 1077, 404-415.
Proc.World Meeting on Acoustic Emission, AEWG, Charlotte NC, 20-23 March 1989.
185 J Wolters "Acoustic emission monitoring of fracture mechanisms in short fibre reinforced thermoplastics: basic studies on model compounds"
Proc.2nd.Int.Symp.Acoustic Emission from Reinforced Composites, SPI, Montreal, July 1986, Session 1, 29-36.
186 M Shiwa, M Enoki, T Kishi and S Kohara "Acoustic emission during tensile loading-holding and unloading-reloading testing in fibreglass-epoxy composites"
Proc.2nd.Int.Symp.Acoustic Emission from Reinforced Composites, SPI, Montreal, July 1986, Session 2, 44-49.
187 M Cherfaoui, A Lemascon, J Roget and D Noiret "Detection and evaluation of defects in unidirectional FRP by acoustic emission monitoring of bending tests"
In K Yamaguchi, K Aoki and T Kishi (editors): 'Progress in Acoustic Emission III'.
Proc.8th.Int.Acoustic Emission Symposium (IAES 8), JSNDI, Tokyo, 21-24 October 1986, pages 586-593.
188 K Yamaguchi, H Oyaizu, K Kudoh and Y Nagata
"Acoustic emission waveform characteristics from FRP during tensile test"
In K Yamaguchi, K Aoki and T Kishi (editors): 'Progress in Acoustic Emission III'.
Proc.8th.International Acoustic Emission Symposium (IAES 8), JSNDI, Tokyo, October 1986, pp 594-601.
189 M Dorosh and A Poursatip
"Indirect quantification of damage growth during three-point bend fatigue of GFRP specimens"
Proc.6th.Intl.Conf. Composite Materials (ICCM-VI), London, July 1987, volume 4, 40-53.
190 R Hill, A Cowking and WS Carswell "An acoustic emission study of stress corrosion cracking in GFRP"
Proc.4th.European Conference on Non-Destructive Testing, London, October 1987, 2872-2880.
191 N Inoue, K Sakakida, F Yamashita, S Inoue, T Hirai, T Katayama and M Hayashibara
"Acoustic emission source location during tensile test of cortical bone"
In K Yamaguchi, I Kimpara and Y Higo (editors): 'Progress in Acoustic Emission IV'.
Proc.9th.International Acoustic Emission Symposium (IAES-9), JSNDI, Kobe, November 1988, pages 177-184.
192 D Rouby "Acoustic emission: a microinvestigation technique for interface mechanisms in fibre composites"
Journal of Acoustic Emission, 1990, 9(2), 117-121.
Proc.3rd.Int.Symp.Acoustic Emission from Composite Materials, ASNT, Paris, 17-21 July 1989, 313-322.
193 T Weng, A Hiltner and E Baer
"Damage analysis in reinforced LCP composites by acoustic emission location techniques"
Journal of Composite Materials, January 1990, 24(1), 103-121.
194 T Nishikawa, T Ishida, M Higuchi and K Kubomura
"Application of an acoustic emission technique to the single fibre composite test"
In K Yamaguchi, H Takahashi and H Niituma (editors): 'Progress in Acoustic Emission V'.
Proc.10th.Int.Acoustic Emission Symposium (IAES 10), JSNDI, Sendai, 22-25 October 1990, pages 567-573.
195 MP Kelly, DO Harris and AA Pollock
"Detection and location of flaw growth in metallic and composite structures"
ASTM Special Technical Publication, 1975, STP 571, 221-240.
Proc.Symp.Monitoring Structural Integrity by Acoustic Emission, ASTM, Fort Lauderdale, January 1974.
196 CD Bailey, JM Hamilton and WM Pless "Acoustic emission of impact damaged graphite-epoxy composites"
Materials Evaluation, May 1979, 37(6), 43-48+54. Spring Conference, ASNT, Phoenix AZ, March 1977.
197 CD Bailey, SM Freeman and JM Hamilton
"AE monitors damage progression in graphite epoxy composite structure"
Materials Evaluation, August 1980, 38(8), 21-27. 38th Fall Conference, ASNT, Denver CO, October 1978.
198 AMG Glennie and J Summerscales "Acoustic emission source location in orthotropic materials"
British Journal of Non-Destructive Testing, January 1986, 28(1), 17-22.
20th Ann Conf, Br Inst NDT, Erskine, September 1985.
199 J Summerscales "A new model for the wavefront profile in unidirectional fibre- reinforced composites"
British Journal of Non-Destructive Testing, October 1992, 34(10), 491-493.
200 EO Ibitolu and J Summerscales "Acoustic emission source location in bidirectionally reinforced composites, Part 1: source location algorithm"
4th.Euro.Conf.Non-destructive Testing, London, September 1987.
Pergamon, Oxford, January 1989, v4, 2881-2891.
201 EO Ibitolu and J Summerscales "Acoustic emission source location in bidirectionally reinforced composites, Part 2: wavefront profile and elastic modulus"
2nd.Int.Conf.Testing, Evaluation and Quality Control of Composites. Guildford, September 1987.
Butterworth Scientific, Guildford, 1987, pp 128-133.
202 DJ Buttle and CB Scruby "Acoustic emission source location in fibre reinforced plastic composites"
Journal of Acoustic Emission, Oct-Dec 1988, 7(4), 211-223.
Harwell Laboratory report AERE R 13039, June 1988.

203 "E04GEF - NAG Fortran Libray Routine Document"
Numerical Algorithms Group NAGFLIB:1655/0:Mk11, November 1983.
204 PE Gill and W Murray "Algorithms for the solution of non-linear least squares problem"
SIAM Journal on Numerical Analysis, October 1978, 15(5), 977-992.
205 CB Scruby Private communication, 4 October 1991.
206 B Castagnede, W Sachse and KY Kim "Optimisation de la localisation d'une source ponctuelle d'emission acoustique dans un materiau anisotrope homogene"
C.R.Acad.Sci.Paris, 1988, 307(II), 1473-1478.
207 B Castagnede, W Sachse and KY Kim
"Localisation de sources d'emission acoustique dans un materiau composite"
C.R.Acad.Sci.Paris, 1988, 307(II), 1595-1600.
208 A Bouheraoua "An accurate acoustic emission location method adapted for composite materials"
In J Boogaard and GM Van Dijk (editors):
Proc.12th.World Conf. Non-Destructive Testing, Amsterdam, April 1989, volume 1, 466-470.
209 A Bouheraoua "An accurate acoustic emission location method adapted for composite materials"
Proc.3rd.Int.Symp.Acoustic Emission from Composite Materials,
Paris, July 1989, Session 14 @ 10:00, pages 375-379.
210 JW Whittaker, WD Brosey, O Burenko and DA Waldrop "Acoustic emission wave propagation and source location in small, spherical composite test specimens"
Journal of Acoustic Emission, 1988, 7(1), 31-40.
211 B Castagnede, W Sachse and KY Kim "Location of pointlike acoustic emission sources in anisotropic plates"
J Acoustical Society of America, September 1989, 86(3), 1161-1171.
212 PG Ciarlet 'Introduction a l'analyse numerique matricielle et a l'optimisation'
Masson, Paris, 1982, 167-207.
213 {Jacobi method in} WH Press, BP Flannery, SA Teukolsky and WT Vetterling
'Numerical Recipes: The Art of Numerical Computing" Cambridge University Press, New York, 1986, 240-246.
214 CARP and CH Adams
"Recommended practice for acoustic emission testing of fiberglass reinforced plastic tanks/vessels"
Proc.37th.Annual Technical Conference, SPI RP/CI, Washington DC, January 1982, session 27-A, 1-13.
215 "Standard practice for acoustic emission examination of fiberglass reinforced plastic resin (FRP) tanks/vessels"
American Society for Testing and Materials standard E1067-85, 31 May 1985.
216 "Acoustic emission examination of fiber reinforced plastic vessels"
ASME Boiler and Pressure Vessel Code Section V article 11, ASME, New York, June 1985.
217 "Fibre-Reinforced Plastic Pressure Vessels"
ASME Boiler and Pressure Vessel Code Section X, ASME, New York, 1995. ISBN 0-7918-2421-7.
218 MA Droge "Discussion: Recommended practice for acoustic emission testing of reinforced thermosetting resin pipe (RTRP)"
Proc.1st. Int.Symp. Acoustic Emission from Reinforced Composites,
SPI, San Francisco, July 1983, session 4 @ 3:25, pages 1-17.
219 "Practice for acoustic emission examination of reinforced thermosetting resin pipe (RTRP)"
American Society for Testing and Materials standard E1118-86, 1986.
220 FH Pickering "Design of high pressure fibreglass downhole tubing: a proposed new ASTM specification"
Proc.1st.Int.Symp.Acoustic Emission from Reinforced Plastics,
SPI, San Francisco, July 1983, Session 4 @ 4:00, pages 1-11.
221 C Oney and FH Pickering "Acoustic emission testing and API standards for fibreglass pipe"
Proc.4th.Tech.Conf.Corrosion and Construction, SPI, Las Vegas, April 1985.
222 "Specification for reinforced thermosetting resin tubing"
American Petroleum Institute, proposed specification 15AR, 1987.
223 "Standard test method for acoustic emission for insulated aerial personnel devices"
American Society for Testing and Materials standard F914-85, May 1985.
224 PJ Conlisk "Acoustic emission testing of RP grating"
Proc.1st. Int.Symp. Acoustic Emission from Reinforced Composites,
SPI, San Francisco, July 1983, session 4 @ 4:30, pages 1-5.
225 SJ Slykhous "Using location and waveform capture to investigate RTR tubing"
Proc.1st. Int.Symp. Acoustic Emission from Reinforced Composites,
SPI, San Francisco, July 1983, session 1 @ 11:30, pages 1-12.
226 TJ Fowler "Calibration and cross-calibration of AE instrumentation using the CARP procedures"
Proc.1st. Int.Symp. Acoustic Emission from Reinforced Composites,
SPI, San Francisco, July 1983, session 5 @ 9:45, pages 1-4.

227 DJ McNally and JR Mitchell "Inspection of composite rocket motor cases using AE"
Proc.40th.Ann.Conf., Reinforced Plastics/Composites Institute,
SPI, Atlanta GA, January/February 1985, Session 5-A.
228 DJ McNally "Inspection of composite rocket motor cases using acoustic emission"
Materials Evaluation, May 1985, 43(5), 728-732+739.
229 GS Whalley and PT Cole
"Development of acoustic emission techniques for quantitative use on aerospace CFRP structures"
Proc.1st. Int.Symp. Acoustic Emission from Reinforced Composites,
SPI, San Francisco, July 1983, session 4 @ 2:00, pages 1-7.
230 "British Aerospace use Dunegan Dart in testing of advanced carbon fibre wings for new experimental aircraft"
Dunegan PAC Limited Applications News, November 1985, (4).
231 J Rodgers "Acoustic emission monitoring of a graphite/epoxy wing segment during limit load testing"
In H Onoe, K Yamaguchi and H Takahashi (editors): 'Progress in Acoustic Emission II'.
Proc.7th.International Acoustic Emission Symposium (IAES 7), JSNDI,
Zao, 23-26 October 1984, 480-487.
232 J Rodgers "Acoustic emission monitoring of flaw growth in a graphite/epoxy experimental wing segment"
Journal of Acoustic Emission, 1985, 4(1), 1-8.
233 J Rodgers "Location and characterisation of flaw growth in aerospace composite structures using AE monitoring"
Hartford Steam Boiler Inspection Technologies paper B5, no date.
234 TJ Holroyd and PE Cox
"An approach to AE monitoring during the rig shop testing of large CFRP aero-engine components"
Proc.2nd. Int.Symp. Acoustic Emission from Reinforced Composites,
SPI, Montreal, July 1986, session 6, pages 189-192.